NONDESTRUCTIVE TECHNIQUES IN INSTRUMENTAL NEUTRON ACTIVATION ANALYSIS

A Dissertation presented to the University of Zambia in partial fulfilment for the award of the Degree of Master of Science in Physics

by

Frank Chisela

October 1979

ABSTRACT

The need to determine constituent elements in materials so as to meet various technological demands in many fields is of an extreme importance. This work is an attempt to establish the efficacy of using non-destructive neutron activation methods based on instrumental gamma-ray spectrometry for the determination of elements in a number of selected materials. Essential aspects of both conventional (i.e. delay) and neutron capture gamma-ray (i.e. "prompt") activation analysis are discussed. Application of the conventional mode is demonstrated in the analysis of Reference Materials and hair samples using short-lived isotopes. Seven chemical compounds are analyzed via neutron capture gamma-ray determination and the detection limits of seven elements of interest (i.e. Cu, Mg, Fe, Na, S, Mn, Ca) calculated based on the matrix counts produced by the 5 Ci Am/Be neutron source.

Results obtained are compared with literature data where available and are found to agree reasonably well within experimental errors.

ACKNOWLEDGEMENTS

Firstly, I should like to thank my supervisors Antony Egan for his advice and encouragement throughout the course, and Nicholas Spyrou of the University of Surrey, UK, for his most invaluable help and suggestions during the experimental projects and preparation of this Dissertation.

The assistance and permission to use the experimental facilities given to me by both the staff of the University of London Reactor Centre at Ascot and the University of Surrey Physics Department is greatly acknowledged.

I am most grateful to both Gwen Wallace and Sara Deane for their willingness to assist with the typing.

Finally, I should like to express my sincere gratitude to International Atomic Energy Agency, National Council for Scientific Research of Zambia and the Zambian Government for financial assistance via an IAEA twelve months fellowship award.

CONTENTS

CHAPTER 1

1. INTRODUCTION TO ACTIVATION ANALYSIS

1.1 Principles of Neutron Activation Analysis.

Neutron activation analysis is a method for determining isotopes and hence elements and levels of concentration in materials. The method is based on detecting and measuring radiation (i.e. nuclear particles and/photons) emitted from isotopes which are produced by nuclear transformation of elements present in the sample when the latter is bombarded with neutrons. There are two main forms in current usage; "prompt" activation in which gamma-ray photons emitted instantaneously from target isotopes are detected and measured during neutron bombardment, and the radioactivation form which relies on the detection and measurement of delayed radiation resulting from the decay of unstable product isotopes produced in the sample by neutron bombardment. In both cases, the amount of radiation emitted from the product isotope is directly proportional to the amount of the precursor isotope and hence the content of the corresponding element in the sample.

In practice, the process involves analyzing a small part (i. e. sample) taken from the bulk of material under investigation and the results obtained from the sample are then assumed to be representative of the whole material. The determination of elements may be achieved by means of either an absolute or comparison procedure (see Section 4.1). The latter is more often used, being easier and more accurate than the former, since it does not depend on nuclear constants which often have to be determined in separate experiments. When a sample is to be analyzed for one or more elements, a standard sample containing known amounts of these elements is irradiated at the same time as the unknown and the radiation then counted in an identical manner. Comparison of the counting rates in the sample and standard gives the weight of the desired

element in the sample by the following relation:

Weight of element in sample =

$$\frac{\text{(Activity in sample) (weight of element in standard)}}{\text{(Activity in standard)}} \qquad (1)$$

Neutron activation analysis based on the production and counting of radioactive isotopes may, in some cases be carried out with chemical separation in order to ensure radiochemical purity of the desired radioelement. Usually, this means subjecting the sample to chemical procedures such as ion-exchange, chromatography, liquid-liquid extraction, distillation, precipitation etc., after irradiation and subsequently counting the radiation. These procedures have a major disadvantage of being time consuming and generally reduce the accuracy of the measurements due to extensive sample handling. However, activation analysis can be particularly simple when the activity can be measured directly on the irradiated sample. This study is concerned with Instrumental nondestructive activation analysis techniques.

1.1.1 The (n,γ) reactions

When a sample is bombarded by neutrons, a number of nuclear reactions may take place. The interaction of neutrons with nuclei is a random process and can only be expressed in terms of statistical probability. The relative probability of a particular interaction giving rise to any one reaction is given by the "reaction cross section" measured in units of area, and conventionally called the barn (1 barn = 10^{-24} cm^2). There are several factors which influence the cross section of a given reaction, but the two most important ones are the energy of the neutrons and the nature of the target nucleus in question.

Neutron interactions which lead to nuclear reactions of the (n,γ) type are the most important ones in neutron activation analysis. Thermal neutrons are known to interact with nuclei predominantly through (n,γ) capture reactions and, therefore, are frequently used as bombarding particles. In (n,γ) reactions involving thermal neutrons, a neutron is captured by a target nucleus forming an excited compound nucleus with an excitation energy equal to the neutron separation energy of 6 to 8 MeV. According to the Statistical Model (20), the compound nucleus has bound energy levels and therefore the excitation energy is insufficient to allow de-excitation by particle emission. Consequently, the excess energy is dissipated by the emission of photon radiation or by the competing process of internal conversion. In fact, the relative frequency of these and other forms of de-excitation is defined by the corresponding partial level widths in the compound nucleus (i.e. radiation widths), and thepartial width for photon emission is given by:

$$\Gamma_\gamma = \hbar/\tau \qquad (2)$$

where τ is the mean lifetime (s) of the excited state,
and $\hbar$ is Planck's Constant ($\hbar = 1.055 \times 10^{-34}$ Js).
For slow neutrons, $\Gamma\gamma$ is of the order of 0.lev, hence τ is of the order of 10^{-14}s for prompt emission of gamma-rays.

The production of radioactive nuclides by (n,γ) reactions is a consequence of the fact that the prompt gamma-ray emission or internal conversion does not remove all of the excitation energy leaving the product nucleus unstable. This eventually decays by β-emission accompanied by one or more characteristic gamma-photons. The gamma radiation resulting from this decay is detected and used for conventional (i.e. delay) activation analysis. A typical decay scheme is shown in figure 1 for ^{28}Al isotope.

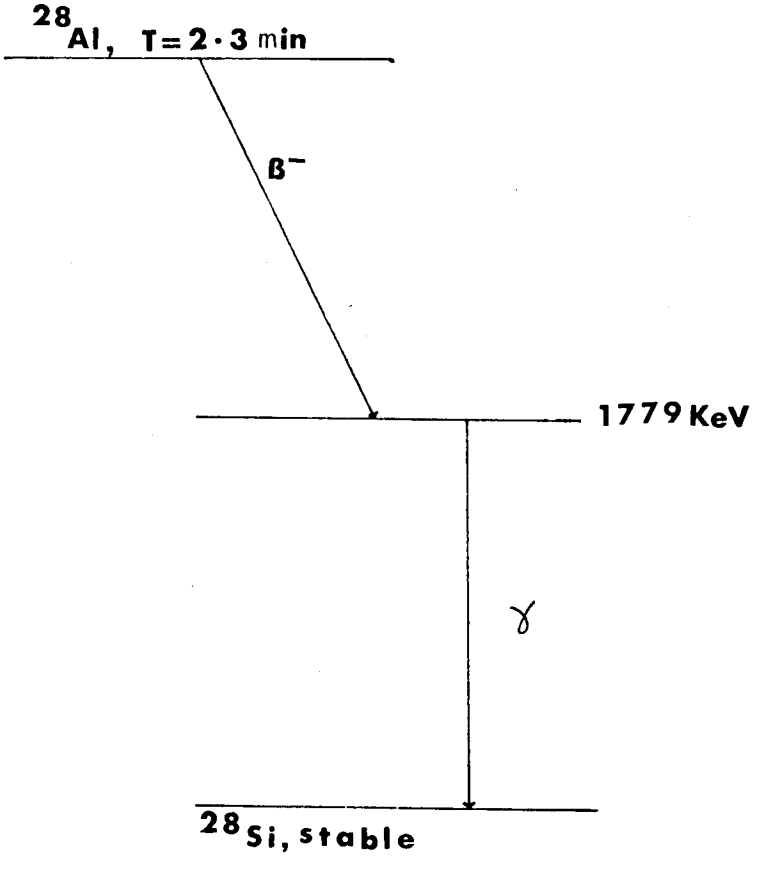

FIG 1 Decay scheme of ^{28}Al

1.1.2 Detection of induced radiation.

The growth of activity for a particular radioactive product in a sample undergoing neutron irradiation is given by P, and

$$P = \frac{mN_A\phi\sigma f}{A_w}(1 - e^{-\lambda t_i}) \qquad (3)$$

where, N_A - avogadro's number (6.02×10^{23} at./g. at.)

ϕ - neutron flux (neutrons/cm^2-s)

σ - cross section for the reaction to take place (barn)

m - total mass of element under investigation (grams)

A_w - atomic weight of the element ($g.gmol^{-1}$)

f - natural isotopic abundance of target nuclide

λ - decay constant of radioactive isotope produced (s^{-1})

t_i - time of irradiation (s)

The detection of photons is performed by means of either NaI (Tl) scintillator or a semiconductor detector such as Lithium-drifted Germanium, Ge(Li) or Lithium-drifted Silicon, Si(Li). The mechanism of detection is a consequence of the gamma photon interaction with the atoms of the detector material. Three main types of interactions can be distinguished:

(a) photoelectric

(b) Compton scattering

(c) pair - production

The photoelectric process is the transfer of the total gamma-ray photon energy to an orbital electron, with the latter being released in the process. On the other hand, the Compton scattering involves a step-by-step loss of the gamma-ray photon energy by the photon to atomic

electrons. In Pair-production, a high energy (≥1.02 MeV) gamma-ray photon is converted into an electron and a positron, the excess energy being shared between the two particles. The positron, within a very short time (10^{-7}-10^{-10}s) (20), interacts with an electron and annihilates producing, in order to conserve linear momentum, two oppositely directed gamma-ray photons of energy 0.51 MeV. Another type of interaction, particularly significant to low energy photons is the Rayleigh scattering which is a form of coherent elastic scattering.

In activation analysis, interest is mainly directed at photo-electric processes since they are representative of the total energy of the incident photon. The other types of interaction become useful when the remaining radiation energy is immediately absorbed by the photoeffect. The amount of an element can then be computed from the photopeak area of its gamma-ray. The photopeak area is given by equation 4 :

Peak area (number of counts)

$$= \frac{mN_A\phi\sigma f\varepsilon_\gamma I_\gamma}{A\lambda}(1-e^{-\lambda t_i})(e^{-\lambda t_w})(1-e^{-\lambda t_c}) \qquad (4)$$

where, I_γ- abundance of the branching ratio of gamma-ray transition

ε_γ- full-energy peak efficiency of the detector for the gamma-ray being detected

t_w- time between end of irradiation and start of counting(s)

t_c- time of counting(s)

and the other symbols remaining as in equation 3 .

1.2 Cyclic Activation Analysis (CAA)

In the conventional application of neutron activation analysis,

a sample is exposed to a neutron flux for a single irradiation preset time. The spectrum can be collected during this irradiation period and analyzed later in the case of "prompt" gamma-ray spectroscopy. Alternatively, the sample may be withdrawn from the flux and the induced activity then counted for a suitable period when the decay mode is used. Cyclic activation analysis is a repetition of the above procedure for a number of cycles, employing the same sample, the counts being accumulated in each cycle to give rise to a larger total activity. The most striking feature of the technique is its capability to depress the background activity compared to conventional irradiation.

The technique was originally suggested by Givens et al (11) in their neutron experiment for remote elemental analysis of lunar and planetary surfaces. It provides an effective means of enhancing detector response for the isotope of interest when the induced radioactivity produced by a single irradiation is of low intensity. But, perhaps the most useful application of the technique is in the assay of elements through short-lived radioisotopes in which activities have half-lives too short for the conventional method. In certain cases, a given nuclide may have nuclear properties which do not permit assaying the element via a long-lived radionuclide. For instance, a short-lived nuclide may be the only radioactive specie produced from the element of interest and which can be assayed without chemical separation (e.g. ^{207m}Pb, T = 0.8 s) (1). Furthermore, a short-lived nuclide may provide the best means of determining an element if the activity of its long-lived radionuclide is riddled with interfering matrix activities (e.g. ^{24}Na, $T_{\frac{1}{2}}$ = 15.0 hr, E_γ = 1368.4 keV and ^{24}Na, $T_{\frac{1}{2}}$ = 20 ms, E_γ = 472,0 keV).

1.2.1 Theory

The most important objective in cyclic activation analysis is to increase the signal-to-noise ratio in order to obtain an improved sensitivity of measurement. Considerable improvement in the sensitivity of measurement can be achieved by repeatedly cycling the sample between the source and the detector for n consecutive irradiate-transfer-count and return cycles, accumulating the counts registered in the detector in each cycle. This means that the detector response to radiation during the second counting period is due to residual activity from the first irradiation plus additional activity produced during the second irradiation period and so on. The mathematical representation of the process is given in equation 5 . The activity of the isotope as a function of time during cyclic activation is shown in figure 2.

The detection of a photon as the full-energy peak in the first counting cycle is given by the activation equation as follows:

$$D_1 = \frac{N\sigma\phi\varepsilon I}{\lambda} (1-e^{-\lambda t_i}) (e^{-\lambda t_w}) (1-e^{-\lambda t_c}) \qquad (5)$$

where D_1 - number of counts

N - number of target nuclei in the sample

σ - reaction cross section

ϕ - neutron flux

ε - detector efficiency

λ - decay constant for the isotope of interest

I - intensity of radiation of interest

and the other symbols remain as in equation 4 .

If T is defined as the cycle period, with the condition that $T \geq t_i+t_w+t_c$, then the detector response for the second counting period is

$$D_2 = D_1 + D_1 e^{-\lambda T} \qquad (6)$$

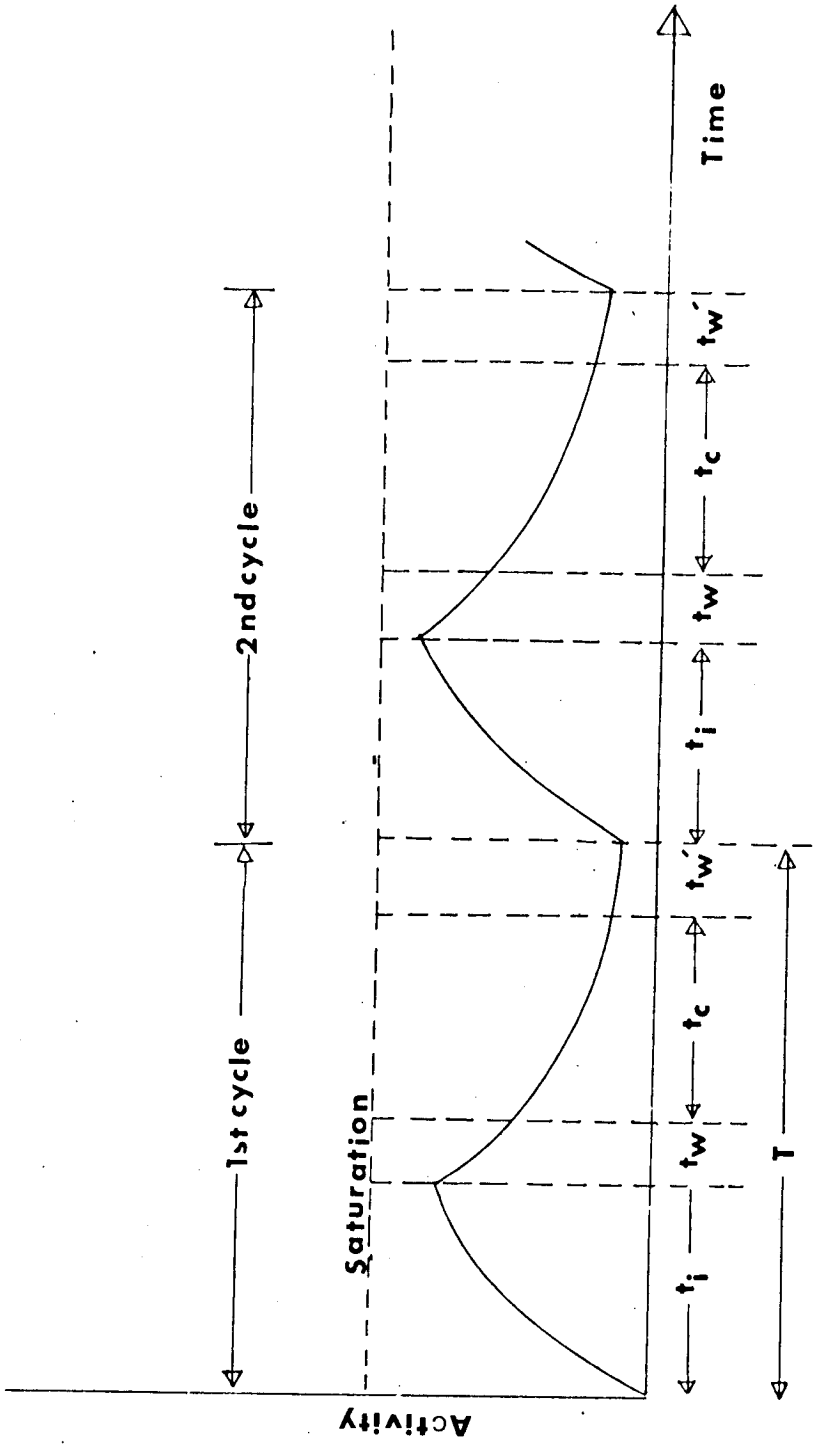

FIG 2

Isotope activity during cyclic activation

and for the n-th counting period

$$D_n = \frac{N\sigma\phi\varepsilon I}{\lambda}(1-e^{-\lambda t_i})(e^{-\lambda t_w})(1-e^{-\lambda t_c})\frac{(1-e^{-n\lambda T})}{(1-e^{-\lambda T})} \qquad (7)$$

The cumulative detector response for all n periods is simply the sum of the individual cycle responses i.e.

$$D_c = \sum_{i=1}^{n} D_i \qquad \text{(n being the cycle number)}$$

and

$$D_c = \frac{N\sigma\phi\varepsilon I}{\lambda}(1-e^{-\lambda t_i})(e^{-\lambda t_w})(1-e^{-\lambda t_c})\left|\frac{n}{(1-e^{-\lambda T})} - \frac{e^{-\lambda T}(1-e^{-n\lambda T})}{(1-e^{-\lambda T})^2}\right| \qquad (8)$$

For a given radioisotope of interest, D_c can be maximized by choosing suitable irradiation, transfer, and counting times. And in particular, for any given total experiment time, nT, the maximum value of D_c occurs when the transfer times are zero, i.e. $t_w = 0$ and $t_i = t_c = T/2$. Figure 3 shows an example of the variation of D_c with the cycle period T for the ^{49}Ca ($T_{\frac{1}{2}}$ = 522 s) and ^{37}S ($T_{\frac{1}{2}}$ = 306 s) isotopes for a total experiment time of 1252 s and 734 s respectively with $t_w = 0$ [19]. It is clea from the graph that there is no point in cycling the sample beyond a certain amount of total time, as D_c only remains constant over an optimum period consistent with the half-life of any given isotope. A comparison of detector response as a function of total experiment time of cyclic and conventional analysis for ^{28}Al ($T_{\frac{1}{2}}$ = 2.31 min) as calculated by Givens (11) is shown in figure 4.

A more rigorous discussion of cyclic activation analysis, including the effect of background, transfer and waiting times on the detector response is presented in reference (12).

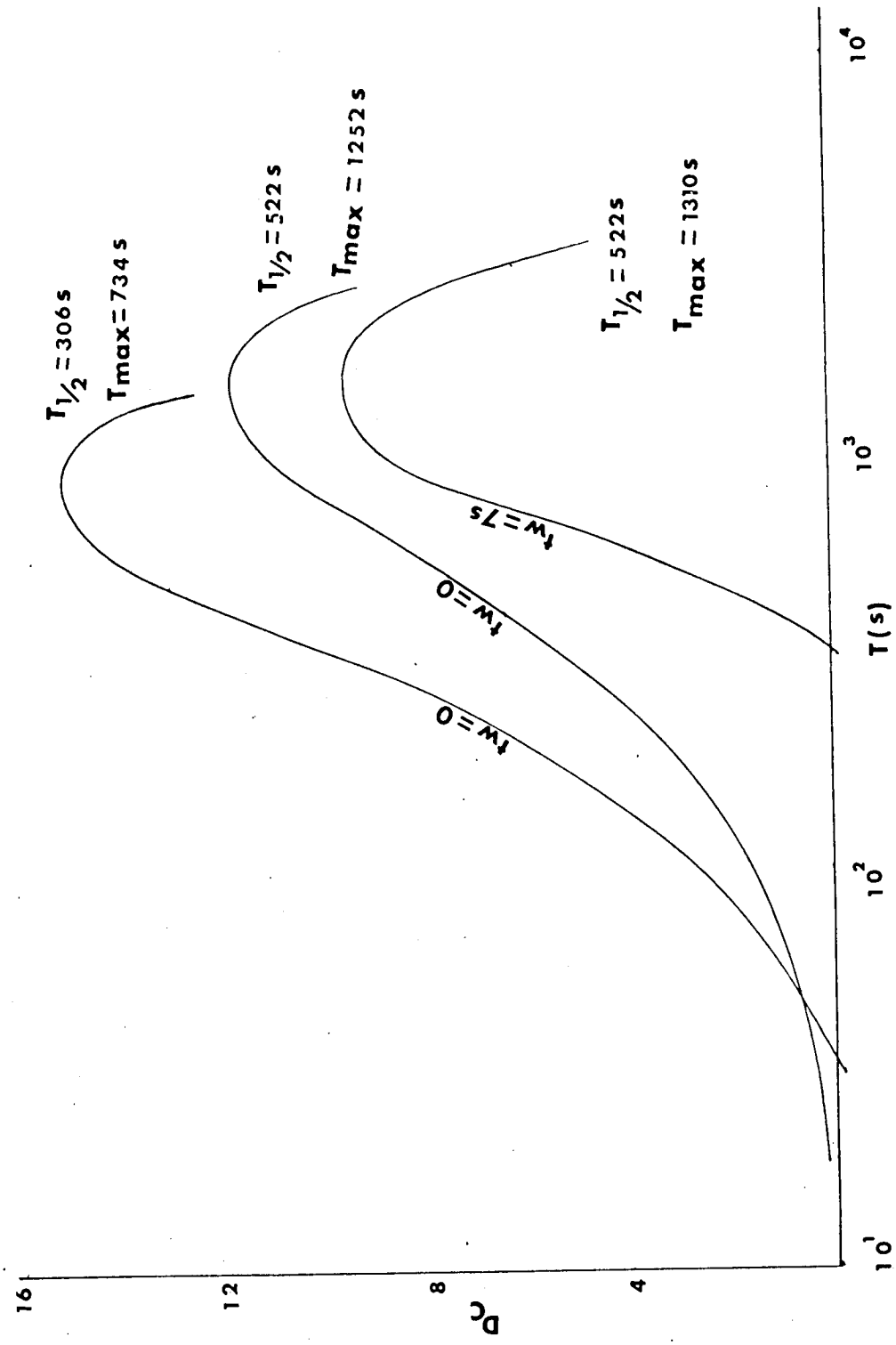

FIG 3

Variation of detector response with cycle period T for ^{49}Ca and ^{37}S isotopes

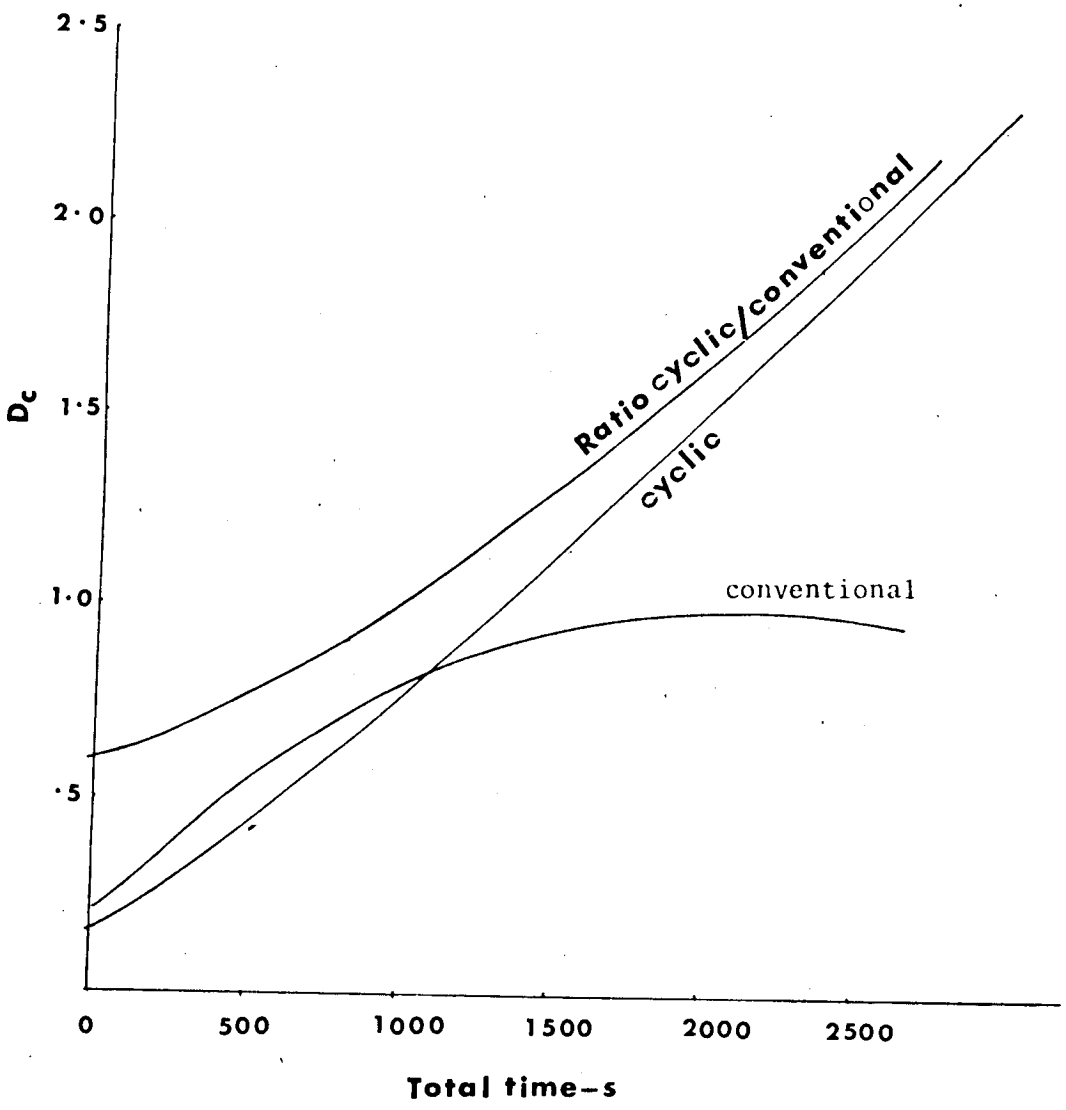

FIG 4

Theoretical detector response for cyclic and conventional activation analysis for ^{28}Al : conventional conditions - ti = tc = T/2, cyclic conditions - t_i = ·009 sec = t_c

T = ·018 sec.

1.3 Radiative Capture gamma-ray analysis

Radiative capture gamma-ray analysis is an alternative technique in thermal-neutron activation analysis, which is based on the measurement of prompt gamma radiation emitted in neutron capture reactions. When a sample is irradiated with a flux of neutrons, a variety of nuclear reactions will occur. The most probable reaction particularly, with thermal neutrons is the (n,γ) capture reaction. A target nucleus captures a neutron forming an excited compound nucleus which de-excites "instantaneously" (approximately within 10^{-12}s - 10^{-16}s) by the emission of one or more radiative gamma-rays. The formation of a compound nucleus has a resonance characteristic, therefore the emitted gamma radiation has an energy spectrum which is characteristic of the emitting element, thus providing a means for elemental analysis.

Analysis by the capture gamma-ray method provides unique capabilities that are not available or convenient using the conventional decay mode. For instance, some elements are not suitable for radioactivation analysis, because the (n,γ) reaction transforms one stable isotope into another stable isotope of the element in question or into a long-lived radioisotope of low activity. But isotopes always emit useful capture gamma-rays during irradiation. The behaviour of biologically interesting elements such as H, N, B and Cd is a typical example in this respect (13). For certain elements such as phosphorous, pure beta-emitters are produced, and therefore nondestructive analysis is not possible by neutron radioactivation; whereas it can still be performed by capture gamma-ray determination. The main restriction, however, to the possible application of the technique on a routine basis is the need for specialized equipment.

1.3.1 Prompt gamma-ray detection

The detection procedures in 'prompt' activation work are essentially the same as in the conventional delay gamma-ray analysis, except that capture gamma-ray measurements are performed during irradiation. The total number of impulses due to capture gamma-rays during sample irradiation in a given neutron flux is given by equation 9 :

$$P' = \frac{mN_A}{A_w} \phi \varepsilon'_\gamma \sigma' f' I'_\gamma t'_i \qquad (9)$$

where, ε'_γ - detector efficiency for the gamma-ray energy measured

I'_γ - intensity of the measured gamma-ray

σ' - capture cross section (barns)

The rest of the symbols are as in equation 3 .

1.4 Epithermal neutron activation

The energy spectrum of neutrons in a nuclear reactor can be divided into three main parts:

a) A fast fission component consisting of prompt neutrons released in fission reactions. The energy spectrum of these neutrons extends from about 0.075 to 17 MeV and is approximately described by the following function (35):

$$n(E) = (2/\pi e)^{\frac{1}{2}} \sinh(2E)^{\frac{1}{2}} e^{-E} \qquad (10)$$

where n(E) - number of neutrons with energy

E per unit energy interval

b) The resonance or epithermal neutrons which are in the process of slowing down in the moderator, including neutrons of energy below ∿1 eV up to about ∿1 MeV. The epithermal neutron flux is assumed to follow a dE/E distribution in water-moderated reactors.

c) A thermal spectrum consisting of neutrons which are in thermal equilibrium with the moderator. This is usually approximated by a Maxwellian distribution in well-moderated thermal reactors. The functional representation is as follows :

$$dn(E) = \frac{2\pi}{(\pi kT)^{3/2}} \exp(-E/kT) E^{\frac{1}{2}} dE \qquad (11)$$

and n(E) is the number of neutrons of energy E per unit energy interval between E and E+dE.

Most applications of reactor neutron activation analysis are based on irradiations with the whole reactor spectrum. But since many elements have high absorption cross section for thermal neutrons, these analyses are almost entirely based on the activation events arising from (n,γ) reactions induced by the thermal neutron component. In general, however, the (n,γ) reactions induced by epithermal neutrons as well as reactions (to a lesser extent) induced by fast neutrons will contribute significantly to the formation of radioactivities of interest.

The rate at which radionuclides are produced by (n,γ) reactions is dependent on the energy distribution of the neutron flux and the way in which the cross section varies with the neutron energy. For many elements, the cross section is inversely proportional to the neutron velocity (i.e. "$1/v$ law") in the thermal energy region. Whereas some nuclides (e.g. ^{23}Na and ^{45}Sc) have cross sections which follow the $1/v$ law also in the epithermal region, up to the energies where the neutron

flux in a reactor beam is very low, and hence will not significantly contribute to the activation rate; other nuclides, however possess large resonances in the low energy epithermal region varying rapidly with the energy. In irradiations with the whole reactor spectrum, the reaction rate per atom for a given nuclide is expressed as follows :

$$R = \phi_{th}\sigma_o + \phi_{epi}(I + \cdot 44\sigma_o) \qquad (12)$$

where,

ϕ_{th} - thermal neutron flux

σ_o - 2200ms^{-1} neutron cross section

ϕ_{epi} - epithermal neutron flux per unit ℓn E

$\cdot 44\sigma_o$ - contribution from the $^1/_V$ tail in the epithermal region.

I - resonance integral, defined as follows :

$$I = \int_{E_c}^{1MeV} \frac{\sigma(E)\,dE}{E} \qquad (13)$$

and $\sigma(E)$ is the activation cross section as a function of neutron energy, excluding the $^1/_V$ contribution. For nuclides following the $^1/_V$ law in the epithermal region, the resonance integral reduces to zero, and the epithermal contribution to the total reaction rate will be negligible. However, for nuclides with moderate or low thermal neutron cross section and high resonance integrals, epithermal activation events will form a major part in the total reaction rate. Thus in such cases, it would seem better to use only epithermal activation in the analysis provided thermal neutrons are properly removed. Also since Neutron Activation Analysis is a multielemental technique, epithermal activation of certain

isotopes with good resonance cross sections may be profitable when these are present in small quantities and masked by huge activities from the more abundant thermally induced isotopes present in the matrix. Thermal neutrons can be removed by means of absorbers e.g. Cd, which has a very high absorption cross section in the thermal region, and is transparent to neutrons above a certain energy E_c (see Fig 5 on Cd cross section) somewhat dependent on the cadmium foil thickness (Ca. 0·4 eV for 0·7 mm Cd). This 'cadmium cut off' is usually referred to as the upper energy limit of the thermal neutrons, and hence the lower limit of the epithermal neutrons.

The response of a given nuclide to epithermal neutrons in a particular irradiation position is described by the cadmium ration :

$$R_{Cd} = \frac{\phi_{th}\sigma_o + \phi_{epi}(I + 0{\cdot}44\sigma_o)}{\phi_{epi}(I + 0{\cdot}44\sigma_o)} \qquad (14)$$

Very often the cadmium ratio of Gold (^{197}Au) is used as a standard reference in estimating the relative magnitude of the thermal flux component. Once the R_{Cd} of Au is known, the cadmium ratio of any other nuclide in a specific irradiation position, provided that the constants σ_o and I are available for the nuclide in question, can then be calculated using equation 15 :

$$R_{Cd} = 1 + \frac{\sigma_o(0{\cdot}44\sigma_o^{Au} + I^{Au})}{\sigma_o^{Au}(0{\cdot}44\sigma_o + I)}(R_{Cd}^{Au} - 1) \qquad (15)$$

In principle, a case for epithermal activation analysis for a large number of elements can be established by considering the "advantage" factor, defined as follows (21):

$$Fa = \frac{(R_{Cd})d}{(R_{Cd})D} \qquad (16)$$

where d denotes the interfering nuclide, and D the nuclide being determined.

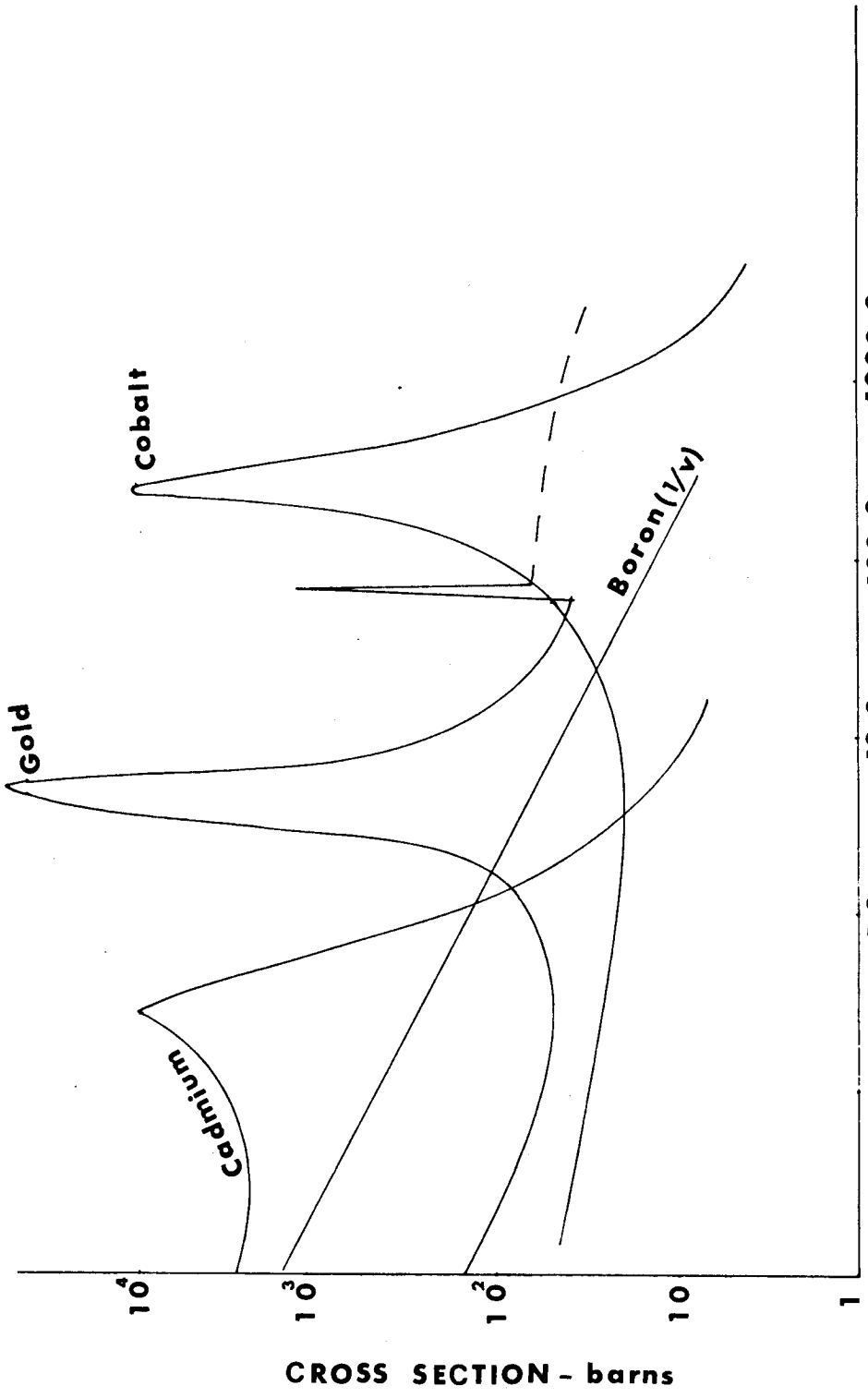

FIG 5

Total cross section as a function of neutron energy for Cd, Au, B and Co

The cadmium ratio of the nuclides can either be determined by experiment in the irradiation position to be used or calculated from equation 15 provided that R_{Cd}^{Au} and the values for the constants σ_o and I are known. For activation analysis with reactor neutrons, the main advantages in the use of epithermal activation are likely to be in the improvement of precision and sensitivity in instrumental activation analysis where elements can be selectively activated with minimum interference. Also, in some cases the amount of activity produced by the nuclide other than the nuclide of interest imposes a practical limit of detection in activation analysis from the standpoint of safety (e.g. ^{24}Na and ^{56}Mn in soils). The high activities from such nuclides can be reduced by epithermal activation as long as the elements being determined have high advantage factors compared to Mn and Na and the latter have small resonances in the epithermal region. And finally the reduction of interference arising from thermal fission of ^{235}U, a parent nuclide for most fission products. Epithermal activation can be used successfully since the fission cross section of ^{235}U shows a $1/v$ dependence. Perhaps the most interesting areas for epithermal activation would seem to be that of enhancing the feasibility of selective activation analysis, whereby the energy distribution of the neutron flux could be changed by introducing suitable filters made from elements of very high cross section in the energy region to be excluded from the neutron spectrum. These filters could be used separately or together with Cadmium. The most important limitation of epithermal activation analysis, particularly using Cadmium is the limited amount of Cadmium that can be placed in an irradiation site close to the reactor without causing reactor operation problems.

CHAPTER 2

2. NEUTRON SOURCES

2.1 Classification of neutron sources

Neutron sources can be classified according to the type of reaction used in the production of neutrons. There are three main sources in current usage;

(a) accelerator-based sources,

(b) isotopic sources,

and (c) reactor neutron sources.

The use of these neutron sources for activation analysis depends a great deal on the requirements of a particular application and the suitability in terms of neutron flux, cost, size and portability of the source.

(a) Accelerator-based sources

There are a number of neutron producing reactions that can be used with accelerator neutron sources. Among the most widely used reactions are the charged-particle-induced reactions in which protons and deuterons bombard various targets. Typical reactions include $^{9}Be(d,n)^{10}B$, $^{3}H(d,n)^{4}He$, $^{2}H(d,n)^{3}He$, $^{7}Li(p,n)^{7}Be$ and $^{2}H(p,n)^{3}He$. The targets are usually constructed in the form of neutron generating tubes which can be inserted in a beam of ions from the accelerators. The neutron fluxes obtained in these accelerators are generally low ($\sim 10^{4}$-10^{8} n $cm^{-2}s^{-1}$) and cannot, therefore, be used for the analysis of submicrogram quantities. The most important function of these sources, however, is the production of monoenergetic neutrons which are used in threshold reactions. The repeated replacement of target tubes, because of their short life expectance ($\sim$ in terms of tens of hours) would seem to reduce the feasibility of using these sources in routine applications.

(b) Isotopic sources

The two most important reactions in radioactive sources are the (α,n) and (γ,n) reactions. In the case of (α,n) reactions, alpha particles are obtained from natural radioactive alpha-emitting isotopes and are made to bombard a light element such as Li, Be and B liberating neutrons. If Be is used as a target element, the reaction producing neutrons is,

$$^{9}Be(\alpha,n)^{12}C$$

The activity of the alpha-emitting radioisotope determines the neutron yield in these sources. Typical sources using this reaction include Po-Be ($\sim 10^{6}$ n/s), Ra-Be ($\sim 1{\cdot}7 \times 10^{7}$ n/s), Pu-Be ($\sim 10^{6}$ n/s), and Am-Be ($\sim 10^{5}$ n/s).

The (γ,n) sources are based on the threshold characteristic of the (γ,n) reaction and usually target materials are elements with low threshold energies for this reaction. Beryllium and deuterium are very often used. A relatively high yield (γ,n) neutron source is the Sb-Be radioactive source capable of producing low energy neutrons ($\sim$·02 MeV) with a total yield of $\sim 10^{10}$ $ns^{-1}g^{-1}$. (17).

An isotopic source which is based on spontaneous fission of heavy nuclei is the Californium -252 (^{252}Cf) spontaneous fission source. On the average, 3·8 neutrons are released in the fission of the ^{252}Cf ($\sim 2{\cdot}34 \times 10^{12}$ $ns^{-1}g^{-1}$) of the source, making it more attractive than the sources discussed above (18). However, the relatively short half-life of ^{252}Cf isotope (2·2 years) works against this advantage.

(c) Reactor neutron sources

There are various types of nuclear reactors which are distinguished by the mode of interaction between the neutrons and the fissile material. However, for the purpose of neutron activation analysis, thermal reactors are the most important source of neutrons. Thermal nuclear reactors are those in which the fission reaction is due to the absorption of slow neutrons; so that a sufficient amount of moderator must therefore be present in the core of the reactor in order to reduce the energies of the fast fission neutrons to thermal energies. In general, 2-3 neutrons are released in the fission of one atom of fuel isotope; so that if an efficient moderating material with a minimum of loss of neutrons via neutron capture or escape from the moderator is used, the surplus neutrons can be used for activation purposes. Although very high neutron fluxes can be obtained from nuclear reactors, the very high cost of building and maintaining one means that they can only be available for use in this respect to those countries which can afford a nuclear research programme.

CHAPTER 3

3. DETECTION

3.1 Essential detector characteristics

The quality of performance in a gamma-ray detector is evaluated in terms of its detection characteristics. The two most important detector characteristics are its detection efficiency and energy resolution and these are almost exclusively determined by the physical properties of the detector material. This follows from the fact that the detection method is based upon the interaction processes which occur within the detector. Almost invariably, suitable detector materials are those in which the probability of interaction is greatly increased as this gives rise to total absorption of the incident gamma-ray photon and hence improved detection characteristics.

3.1.1 Energy resolution

The gamma-ray pulse height distribution resulting from the absorption of discrete energies of gamma-rays does not show discrete spectral lines corresponding to these monoenergetic gamma-rays. Instead it consists of peaks with certain widths corresponding to photoelectric events within the detector and a lower energy continuum resulting from Compton interactions. This broadening of spectral lines is due to the statistical processes in the detector and the associated electronics following the radiation energy transfer to the electrons in the photoelectric effect. Usually the full-energy peaks can be approximated as gaussian photopeaks under the assumption that photoelectric events follow a normal distribution. This means that gamma-rays with energies close to each other will produce overlapping photopeaks in the spectrum.

For good differentiation of various radionuclides and their mixtures after activation, photopeaks of minimum width are required. The energy resolution of a detector is evaluated as the net ratio of the full width at half maximum (ΔE) to the average energy of a given gaussian peak (E).

3.1.2 Detection efficiency

In practice, a detector is just not capable of detecting all the radiation emitted by a given source. This limitation is due to a number of factors, the most important being the physical properties of the detector material, its size and geometry. In general, under specified counting and fixed geometry conditions, the total number of events produced in a detector due to gamma-ray photons of a particular energy represents a constant fraction of the total number under ideal conditions. This fraction can be evaluated as the net ratio of the detected photons to those emitted by the source, thus giving the efficiency of a detector. The simplest method of determining the detector efficiency is by means of accurate calibrated gamma-ray sources (7), although other procedures such as the utilization of known cross sections of reactions can be applied. The efficiency of a gamma-ray detector varies considerably with the gamma-ray energy and source-detector geometry, so that for precision measurements it is always essential to determine the efficiency of the detector in the energy region of interest. Another quantity of interest usually evaluated is the photopeak efficiency, obtained by simply working out the net ratio of counts measured under the photopeak to the total counts in the spectrum.

3.2 Detectors for gamma-ray counting

There are two main types of gamma-ray detectors used in activation analysis (a) scintillation detectors and (b) semiconductor detectors, as

the pulse output from these detectors is proportional to the amount of energy absorbed.

(a) The most widely used scintillation detector is the NaI crystal activated by thallium. In this detector, a gamma-ray photon interacting with the NaI(Tl) crystal will produce a pulse of light that is proportional in magnitude to the amount of energy given to the crystal by the gamma-ray photon. The photocathode of a photomultiplier tube (P.M.) converts this light pulse into a proportional electrical pulse, which is then multiplied further, by a series of secondary-emission multiplying steps at the dynodes of the photomultiplier tube. The electrical pulse is then output to associated electronics for amplification.

The higher atomic number of Iodine (Z = 53) gives the NaI(Tl) scintillation detector a greater photoelectric efficiency owing to the fact that the probability of photoelectric absorption is greatly enhanced for absorber materials of high atomic number Z. In fact, atomic photoelectric cross sections are approximately given by the following equation (36) :

$$\sigma_\tau \approx \text{const.} \times \frac{Z^n}{E_\gamma^3} \qquad (17)$$

where the exponent varies between 4 and 5 depending on incident gamma-ray energy. The large active volume of these detectors also means that the probability for multiple Compton events, followed by photoelectric interaction of the scattered photons will be increased. The energy resolution of the NaI(Tl) is however, not very good. This poor resolution of the NaI(Tl) must be understood in terms of the increased minimum energy required to produce the equivalent of one electron charge. To obtain the equivalent of one electron charge to the output pulse, approximately 300eV is needed in a NaI(Tl) detector. Furthermore, the conversion of radiation

energy into electrical pulses involves a large number of physical processes which have inherent statistical uncertainties associated with them.

(b) Semiconductor detectors are based on the solid state properties of germanium and silicon. The operation of the detector is basically the collection of the charge carriers released in a solid by the absorption of gamma-ray photons. Unlike the NaI(Tl), where a minimum energy of 300 eV is required to produce one photoelectron from the photocathode, only an average energy of 3.6 eV in Si and 2.9 eV in Ge is needed to create an equivalent of one electron charge. This feature is responsible for the excellent energy resolution of semiconductor detectors. For instance, while the resolution of a NaI(Tl) at 661.6 KeV (^{137}Cs gamma-rays) is between 7% and 10%, that for a suitable semiconductor may well be between 0.3% and .5% at the same energy.

There are four basic types of semiconductor detectors, commonly used in activation analysis. They are (1) Silicon-Surface barrier detectors, (2) intrinsic germanium detectors, (3) Silicon-Lithium drifted detectors - Si(Li), and Germamium-Lithium drifted detectors-Ge(Li). The Ge(Li), because of the high Z number of germanium (Z = 32 as opposed to Z = 14 for Si) is almost exclusively used for gamma-ray spectrometry. Silicon based detectors are much better fitted for the use of low-energy gamma-ray, X-ray, and charged particle spectrometry. The major drawback with semi-conductor detectors is that present technological limitations do not allow larger crystals to be made, so that most detectors have very small sensitive volumes giving the detectors very low intrinsic efficiency characteristic.

A small semiconductor detector used for X-rays and low-energy gamma rays in activation analysis is the Intrinsic Germanium Low-Energy

Photon Detector (LEPD). The main advantages for low energy spectrometry (8) are :

(1) the ratio of photoelectric to Compton-interation cross section increases at low energies which has the effect of simplifying the spectra, minimizing the problem of superposition of full energy peaks on the Compton continuum of higher energy radiation.

(2) it is easier to discriminate against high energy radiation by simply varying the thickness of the detector.

(3) absorption coefficients are generally high in the low energy region, hence small detectors allow measurements with improved detection efficiencies.

A practical disadvantage with the Ge(Li) and the intrinsic germamium detector is that they have to be continuously stored and operated at reduced temperatures in order to minimize noise due to leakage current and maintain the stability of the drifted Lithium. Thus all Ge(Li) and Ge (intrinsic) detectors are enclosed in a vacuum cryostat which provides thermal contact between the germanium crystal and a reservoir (dewar) of liquid nitrogen at a temperature of 77K.

Although, in general semi-conductor detectors have more desirable features including high energy resolution, compact size, relatively fast timing characteristics than scintillation detectors, their inferior detection efficiency may outweigh these advantages in certain applications where high efficiency is the dominant consideration. In practice, the question of choosing a detector between the Ge(Li) or a NaI(Tl) for any application is one of considering the detector characteristics in

relation to the requirements of that particular application and the nature of radiation to be measured. A critical evaluation of detector characteristics, comparing a NaI(Tl) with the Ge(Li) detector in low level gamma-ray spectrometry is given in reference 9.

3.3 Instrumentation

The basic equipment for gamma-ray spectroscopy as used in neutron activation analysis consists of six parts :

(1) high-voltage power supply,

(2) detector,

(3) preamplifier,

(4) linear pulse amplifier,

(5) Multichannel Pulse-height Analyzer, and

(6) output device.

A block diagram of a typical assembly is given in figure 6.

(1) High-Voltage Power Supply (H.T.)

The power supply provides the necessary bias-voltage for the detector. Because the efficiency of a detector is a function of the applied bias-voltage, great stability is the main requirement of a power supply.

(2) Detector

Provides the medium in which the interaction processes essential for the detection of radiation occur.

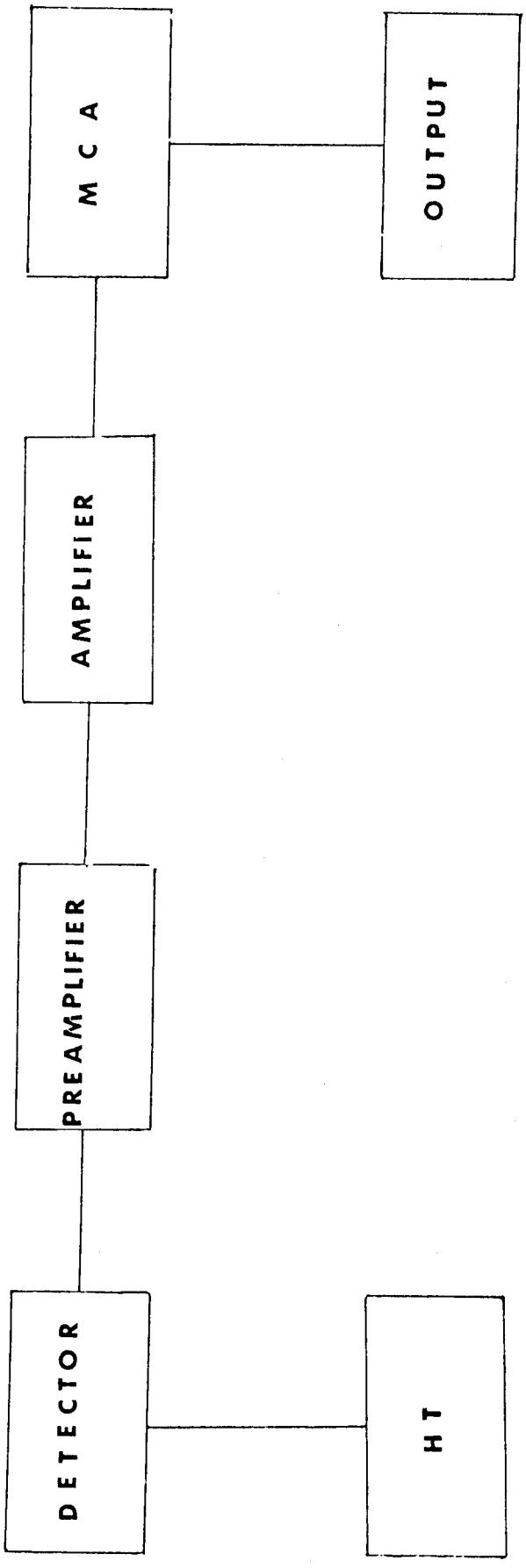

Figure 6

Typical gamma-ray counting equipment

(3) Preamplifier

The output pulses from the detector are generally of the order of few millivolts, and hence they have to be amplified. The signal pulses cannot, however be presented directly to a high-gain amplifier because of the problem associated with the electrical noise at the input stage of the amplifier system. So that almost in all gamma-ray spectrometers a low-noise preamplifier is employed. The most widely used preamplifier, particularly with Ge(Li) detectors is a low-noise charge-sensitive type incorporating a field-effect-transistor (FET) as the input amplifying element.

(4) Pulse amplifier

Apart from providing maximum signal gain ($\sim$1000), the major requirement of an amplifier for use in Ge(Li) gamma-ray spectrometry, is that a choice of proper shaping networks are included to achieve the best signal-to-noise ratio. Additionally other features of importance such as overshoot due to pulse-pile-up problems, amplifier gain stability and amplifier noise as related to the noise level at the output of a preamplifier can be provided for.

(5) Multichannel Pulse-height Analyzer (M.C.A.)

The M.C.A. consists of an analogue-to-digital converter (A.D.C.), an address scaler and a memory block for storage. Essentially, the A.D.C. digitizes the signal pulses from the main amplifier, whereas the address scaler sorts the digital data according to the pulse-amplitude and stores them in corresponding slots (channels) in a ferrite memory core. The channels are updated continuously in the course of a counting experiment providing a simultaneous measurement covering a wide range of energy.

In order to take advantage of the high resolution of the Ge(Li) detectors, multichannel analyzers with at least 1000 channels are required.

(6) Output device

The spectral data from multichannel analyzers can be output in a variety of ways usually depending on the user requirements. As well as usi Cathode Ray-Oscilloscopes, recorders and printers, magnetic discs, and floppy (diskettes) disks, magnetic tapes and paper tapes are used.

3.4 Analysis of gamma-ray spectra

The analysis of NaI(Tl) or Ge(Li) gamma-ray spectra consists of two parts :

(i) qualitative analysis

(ii) Quantitative analysis

(i) Qualitative interpretation typically involves location of photo-peaks in the spectra and determination of their energy accurately. Then identification of the corresponding radionuclides is possible. The identification is usually based on compilations of gamma-ray energy data including branching ratios (in intensity of gamma-rays), other associated energies of an isotope and half-lives so that the process can be made easier by eliminating unlikely products.

(ii) Quantitative analysis, on the other hand includes determination of peak energies, measurement of peak intensities and calculation of concentrations of the elements from which the gamma-ray emitters were formed by one of two methods, as explained in Section 4.1 i.e. comparator or absolute.

3.4.1 Determination of peak areas

The concentration of a given radionuclide in a sample is obtained by computing the area under one of its photopeaks present in the gamma-ray spectrum. When a comparison method is used, a standard sample of known concentration will be activated, treated identically and the corresponding photopeak area determined. Very often, the spectrum obtained after activation contains many photopeaks corresponding to a mixture of radionuclides. In addition to this, a large number of photopeaks in the lower energy region of the spectrum are superimposed on the Compton centinuum of higher energy gamma-rays. Therefore, whatever method is used in determining photopeak areas, it must be ensured that only the photopeak area corresponding to the given radionuclide is evaluated and not the contribution of the continuous spectrum of another radionuclide. Equally important is the amount of background activity subtracted from the Peak as the sensitivity largely depends upon the background activity under the Peak (real background and Compton continuum).

There are many methods used in evaluating peak areas classified in two main groups : the first treats the digital data directly, while the other fits the data to a known function and integrates it to determine the peak area (4).

When using digital data directly, the methods which are mostly used to determine peak areas are (6) :

(a) Total peak area method (TPA) (4) :

$$A = \sum_{i=l}^{i=r} a_i - (a_\ell + a_r)(r - \ell + 1)/2, \qquad (18)$$

where a_i = number of counts in channel i;

ℓ = channel number at left of limit of photopeak-

r = channel number at right limit of photopeak

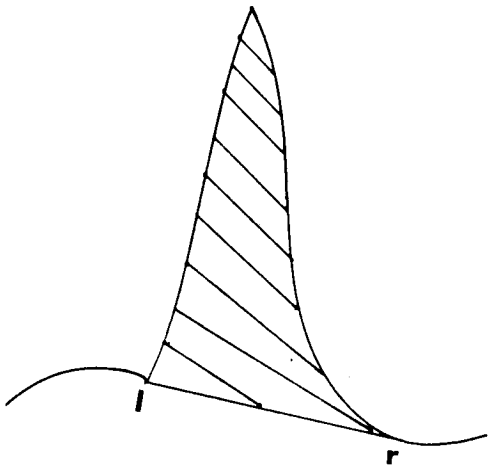

Total Peak Area

(b) A modification by Wasson (4) of the total peak area.

$$A = \sum_{i=-n}^{i=+n} a_i - (n+\tfrac{1}{2})(b_n + b_{-n}) \qquad (19)$$

where n = number of channels on the left and right from the centremost channel,

and b_n = background in channel n from a straight line drawn between channels ℓ and r.

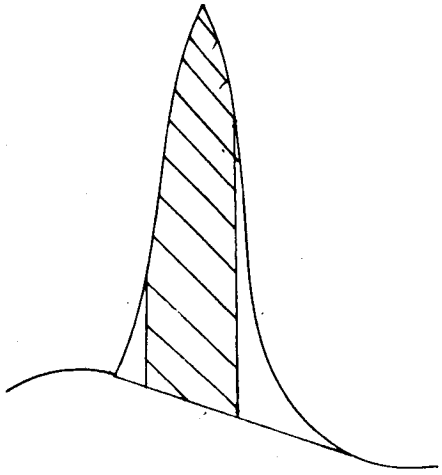

Wasson's modification of the total peak area

(c) Covell's method (15) :

$$A = \sum_{i=-n}^{i=+n} a_i - (n + \tfrac{1}{2})(a_n + a_{-n}) \qquad (20)$$

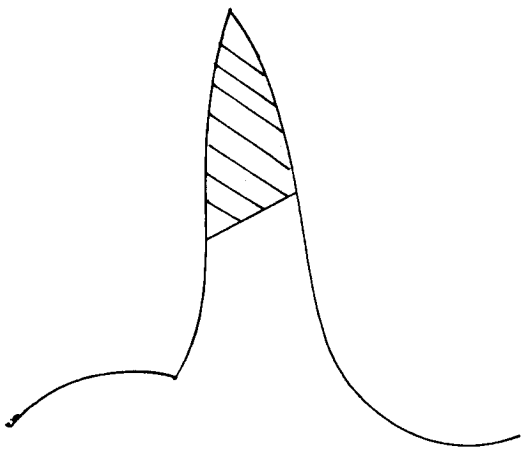

Covell's method

(d) Sterlinski's method (16) :

$$A = na_o + \sum_{j=1}^{n} (n - 2j + \tfrac{1}{2})(a_{-j} + a_j) \qquad (21)$$

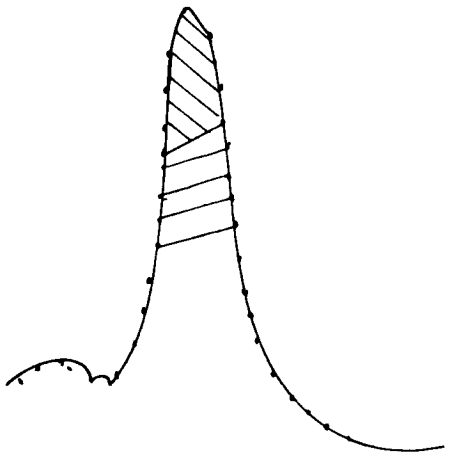

Sterlinski's method

(e) A combination of Wasson and Sterlinski method (4) :

$$A = na_o + \sum_{j=1}^{n} (n-j+1) - (a_{-j}+a_j) - \sum_{j=1}^{n} (j+\tfrac{1}{2})(b_{-j}+b_j) \qquad (22)$$

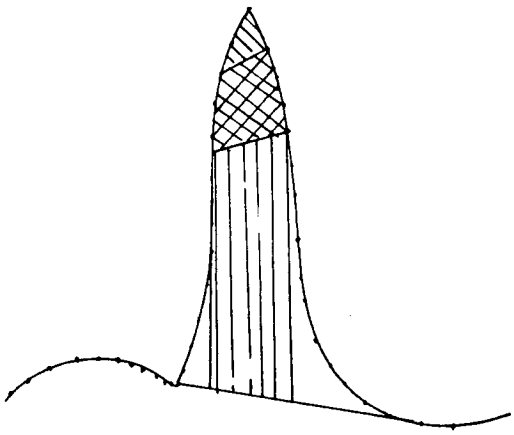

Wasson-Sterlinski method

(f) Quittner's method (5) :

$$A = \sum_{i=-n}^{i=+n} (a_i - C_i) \qquad (23)$$

where C_i is the background in channel i as determined from the expression provided by Quittner :

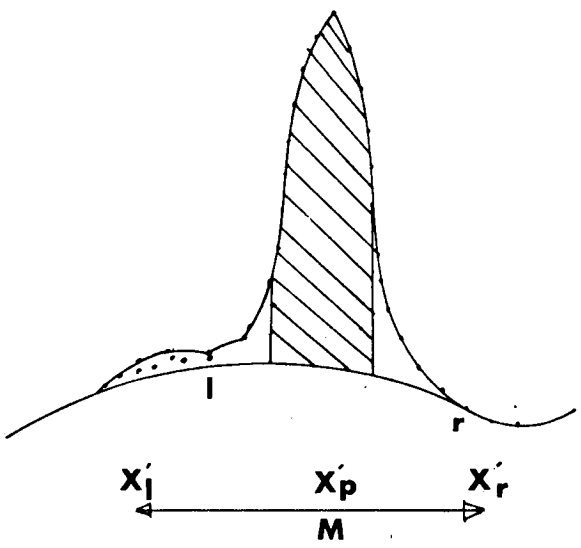

Quittner's method

The main advantage with the total peak area method of integration (a) is that it yields the greatest number of counts for a given peak. Covell's method (c) provides the theoretical advantage of using the channels which have the smallest relative standard deviation. Sterlinski's method (d) is based on the weight of accumulated counts. The major difference between Quittner's method and the other method is that in the former a non-linear base line subtraction is used and the latter employ a linear subtraction.

In the case where spectral data is fitted to a function, the most advantageous method using a computer is the so called the "least-squares method". Essentially, the method is based upon the choice of a suitable function or a combination of functions that fits as perfectly as possible not only the photopeak itself, but also the continuum spectrum under the peak. Usually, the problem formulated in the least-squares sense takes the form :

$$\phi = \sum_{i=1}^{n} \left| \left\{ Y_i - F_i(P_j) \right\} / \Delta Y_i \right\}^2 \qquad (24)$$

and the objective is to minimize ϕ, where Y_i and ΔY_i are the measured value and error respectively, at the i-th data point X_i; and $F_i(p_j)$ is the value predicted by the function used in the fit. Initial estimates of the parameters are supplied as input data. The program then determines the direction and magnitude of the correction vector to the parameters. For most of gamma-ray spectra obtained with Ge(Li) spectrometers, the basic function used as the first approximation for the full-energy photopeak is the Gaussian function for symmetrical peaks with either a linear background or a higher order polynomial. There are numerous computer programs in current usage for the analysis of gamma-ray spectra and one, in particular SAMPO has been used in this work (3).

3.4.2 SAMPO

This is a computer program, originally developed by Routti and Prussin (3) as a photopeak method for the analysis of gamma-ray spectra obtained from semiconductor detectors. A modified version of this program has been implemented by the University of Surrey on the University of London Computing System (2). The method uses a functional representation in which the central part of the photopeak is described by a Gaussia and the tails on either side of the peak by exponential functions. Essentially, the program works by defining a line-shape for each photopeak in the spectrum and then fitting the data around the peak, in the least-squares sense with the functions. The background continuum is represented by a straight-line approximation smoothly varying with the energy. Two options of fitting are available in the program;

(1) values of the shape parameters from the strongest lines in the spectrum (i.e. peak centroid, lower tailing, higher tailing and the peak width all in units of channels) are specified as input to the program through the "SHAPE IN" subroutine. The program then linearly interpolates to define other lines in the spectrum with respect to the channel location;

(2) Peaks are located by a search algorithm (PEAK FIND) and without any assumption of line-shape parameters, the program computes the Gaussian width and the extent of the upper and lower tailing (SHAPEDO) with an estimate of the goodness of fit. Results from the program include the energies and intensities of the photopeaks and the estimated accuracy of these results. The energies are related to channel locations through energy calibration, and the intensities to peak areas through efficiency calibration.

The outstanding feature of the program lies in its versatility to analyze data measured under a wide variety of experimental conditions

accommodating variable statistics, different amplifier gains and detectors of all sizes and performance. In multielement analysis, the ability of the program to handle efficiently complex spectra obtained from Ge(Li) detectors with many peaks, some of them overlapping (i.e. doublets and multiplets) is perhaps one of its most important attributes.

CHAPTER 4

4. APPLICATIONS

4.1 Comparator and absolute methods

(a) Absolute method.

Although in this work,a comparison standard method has been used in all analyses, it is perhaps worthwhile to mention the possibility of employing the absolute methods. The activation relationship given by equation 3.0 consists of two sets of data relating to any activation product, namely the nuclear and experimental data. Absolute elemental masses of target elements can be determined using this equation without recourse to comparison with standards. In fact, for any activation product, the nuclear part of the data (i.e. I,f,N,A,σ,λ) is always a constant and all that is necessary in any analysis is the determination of the experimental part of the data (ε,ϕ,t). However, absolute methods are in general not very popular, mainly because of lack of accurate knowledge of the nuclear constants for many target elements. In addition, the reliability of attaining an accurate weight determination will depend on the accuracy with which the absolute values of the experimental variables (ε,ϕ,t) can be determined.

(b) Comparator method.

Many sources of error can be eliminated by irradiating the sample with a standard of similar composition. When this method is used, both the nuclear and the experimental data relating to a radioisotope formed in the activation are a constant and are simply dropped out in the calculations. Since this method involves preparing the sample and a standard in an identical manner, errors arising from non-uniformity in the sample and the standard, surface contamination providing from dust and the instruments may be introduced.

There are various methods of sample preparation and handling, depending on the physical properties of the material. Solid samples, such as stones, and other mineral materials are usually crushed and made into homogeneous pellets. Organic and biological materials can be ashed at low temperature, reducing losses due to evaporation. A comprehensive discussion of preparation of samples and standards can be found in reference 10. In general, precision and accuracy in activation analysis is a function of several random errors whose origin can be identified with the following factors :

(1) homogeneity and preparation of the sample-

(2) irradiation conditions;

(3) nuclear constants;

(4) measurements of the activities.

If, however a comparator method is used and both the sample and the standard are carefully weighed, irradiated and counted identically, then the overall precision and accuracy should only depend on the statistical error due to the randomness of counting.

4.1.1 Analysis of standard Reference Materials (SRM's)

Certified as well as non-certified standard Reference Materials (SRM's) commonly used to check the accuracy and precision of analytical methods were analyzed using nondestructive instrumental neutron activation techniques. The main objective of the exercise was to study short-lived isotopes characterized in these materials and hence evaluate their practical use in instrumental elemental mass determinations based on the comparator method. A summary of the materials used and the analysis scheme is given in Table 1.

	SRM USED	IRRADIATION AND COUNTING CONDITIONS		
		r_{sd}^{*} 0.5mm	0.5mm	0.5mm
		A	B	C
(i)	NBS ORCHARD LEAVES (1571)	t_i 60 sec	600 sec	1200 sec
(ii)	NBS BOVINE LIVER (1577)			
(iii)	BOWENS KALE	t_w 10-90 sec	60-600 sec	100-1000 sec
(iv)	NBS ARGILLACEOUS LIME			
(v)	NBS FLINT CLAY	t_c 600 sec	100-1000 sec	100-1200 sec

Table 1 : SRM's used under varying t_i, t_w, t_c conditions.

r_{sd} = sample-detector distance

* only for Biological SRM's.

(i) Sample preparation

All standard Reference Materials used were supplied in powder form Several pellets of approximately 6.0 mm in diameter and 2.0 mm thick were made from each Reference Material using contamination-free stainless steel tools. This size was found to be a minimum which gave these pellets an average standard weight of not less than 250 mg, the weight recommended by N.B.S. (22) for the purpose of homogeneity. However, it was not always possible to produce pellets to these dimensions, so that pellets of less or more than 250 mg were also used.

(ii) Irradiations

The University of London Reactor Centre's (U.L.R.C.) 100 KW "Consort II" reactor was used for all irradiations. The reactor is of the swimming-pool type using 24 fuel elements (80% U-235 enriched) which are clad in high purity aluminium. The reactor core is located in an aluminium tank, 7m deep and 1.5m in diameter which also forms the coolant containment. Figure 7.1 shows the reactor core and the beam tubes for irradiations. A summary of reactor irradiation and beam facilities is given in table 2a. The biological shielding is of ordinary concrete of 2.5m thick (see diagram 1). Details of reactor specifications are given in table 2b. The reactor has an In-Core-Irradiation-System (I.C.I.S.) for the irradiation of small samples at high neutron fluxes (maximum thermal flux $\sim 1.7 \times 10^{12} n/cm^2 sec.$) for periods from less than a second up to several hours. The I.C.I.S. is particularly suited for work with short-lived activities since it incorporates a fast pneumatic transfer system (shuttle) which enables samples to be transferred from the irradiation position to a counting room and vice versa within 12 seconds. Figure 7.2 is a fume cupboard constituting the sample-receiving port of the pneumatic system.

Samples of Reference Materials made into tablets (see Section 4.1.1(

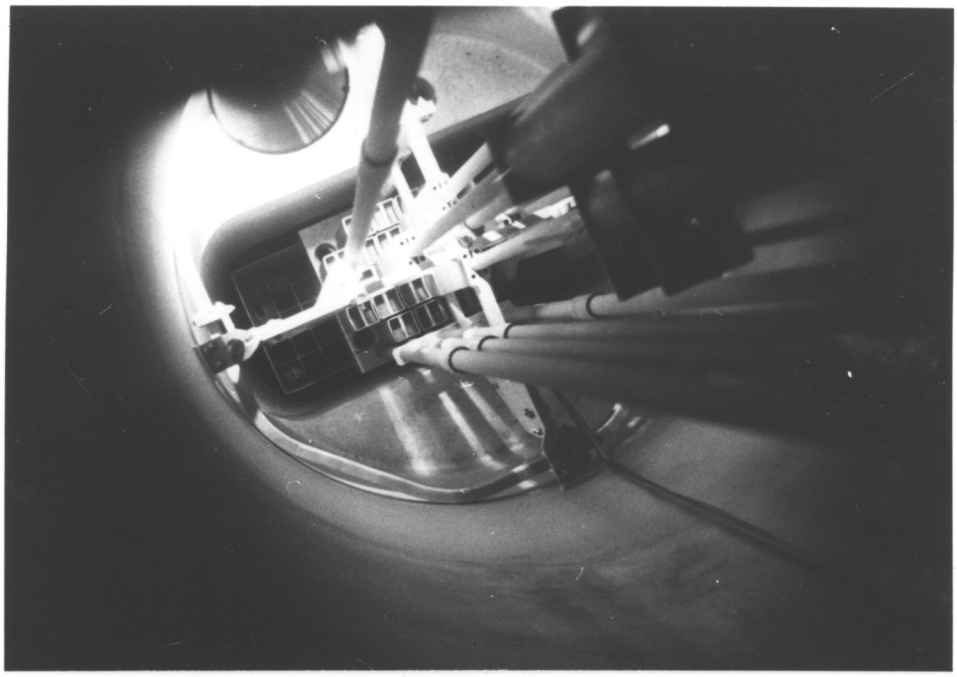

Figure 7.1 University of London "Consort II" reactor core showing the fuel elements and the irradiation tubes.

Figure 7.2 Fume Cupboard for the ICIS pneumatic transfer receiving port.

TABLE 2a.

REACTOR IRRADIATION AND BEAM FACILITIES

Facility	Thermal flux ($n/cm^2.sec$)	Fast flux ($n/cm^2.sec$)
Vertical tube in centre of core (ICIS pneumatic sample irradiation system) (2.5cm. dia.)	1.7×10^{12}	0.9×10^{12}
Vertical tubes (5) at side of core (3.2cm. dia.or 4.8 cm. dia.)	1.3×10^{12} (max)	0.5×10^{12} (max)
Horizontal beam tubes (9) (minimum 15cm. dia.)	3×10^{11} to 3×10^{9}*	10^{11} to 10^{9}*
Vertical tube terminating in graphite near tank (13 cm. dia.)	3.5×10^{10}*	10^{10}*
Thermal column with horizontal and vertical branches (91 x 91cm.)	1×10^{9}*	5×10^{7}*
Vertical thermal column facility	3×10^{8} to 10^{6}	----
Irradiation holes (6) in thermal column (5 at 7.6 x 7.6cm.; 1 at 18 x 18cm.)	1.3×10^{11} (max)	0.8×10^{10} (max)
Bare face thermal column: containing NISUS fast neutron spectrum assembly (91 x 91cm.)	5×10^{10}*	10^{10}*
Through tube (9.5cm. dia.)	5.5×10^{10}*	2×10^{10}*
Beam tube terminating in cave in shield (7.6cm. dia.)	3.5×10^{10}*	10^{10}*

NOTE:

The quoted thermal flux is the Westcott flux and the fast flux is the "equivalent Ni flux". Estimated values are indicated by asterisks.

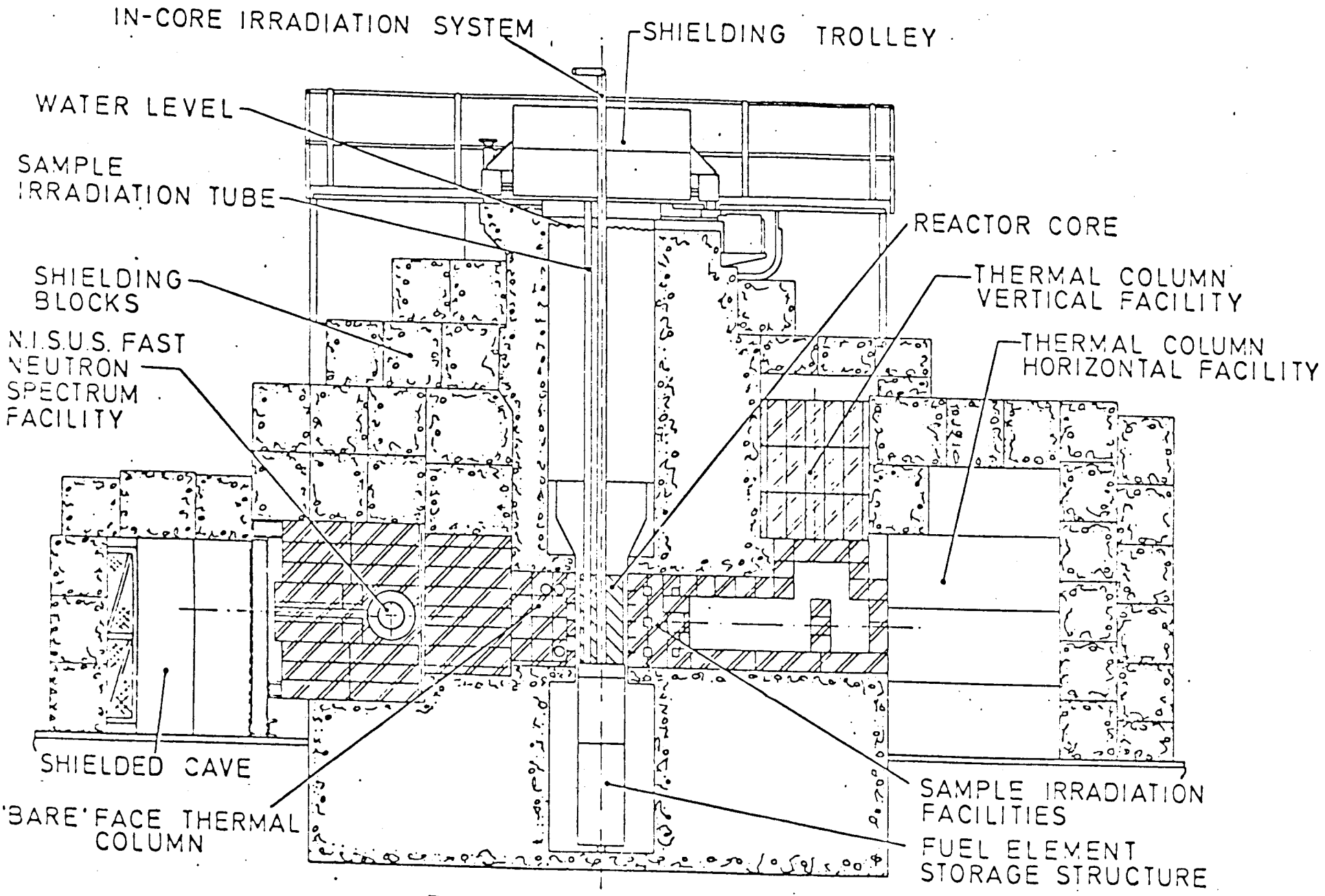

REACTOR EXPERIMENTAL

TABLE **2b**

REACTOR SPECIFICATION

Maximum thermal power	100kW
Fuel elements	Standard MTR type
Plate material	Uranium/aluminium alloy
Enrichment	80% U235
Cladding	Aluminium
Max. no. of plates per element	12 or 16
Wt. of U235 per element (nominal)	138g or 180g
Critical mass (clean core)	3045g U235
Reactor core	
Geometry	24 elements in parallelepiped
Operating mass of U235	3265g (typical)
Excess reactivity	1.0% (typical)
Moderator, coolant and reflector	Light water
Control rods	
Material: safety and coarse rods	Cadmium sheathed in stainless s
fine rod	Stainless steel
Reactivity worth:	
fine rod	0.5%
coarse rods (2)	1.4% and 2.2%
safety rod	2.2%
Coolant flow	9000 litres/hour
Max. temperature rise (inlet/outlet)	$10^{o}C$

were encapsulated in thin-walled low density polyethlene vials and then placed into another vial suitable for I.C.I.S. irradiation. At least three samples of each material were irradiated under three modes of irradiation shown in table 1. Immediately after irradiation, samples were transferred into clean vials ready for counting. This was necessary to avoid counting activity produced in the container material.

(iii) Counting All biological samples were counted at a fixed geometr with only the 0.5mm thick standard Whatman filter paper between the detector surface and the sample. Because of the relatively higher activity induced in geological samples, they were counted at a fixed geometry of 5cm above the surface of the detector. These two values for t sample-to-detector distance were determined so that the dead-time was below 30% and no distortion in the photopeaks occured. The counting equipment consisted of a 42 cm^3 Ge(Li) detector which was coupled to a 1412 Canberra Research Amplifier and an MCA Laben 8000 system of 4096 channels with a Magnetic Tape Interface of fast print readout modes (see figure 7.3). The System was calibrated at 1.0 KeV/channel with a maximum tolerable drift of 0.2%/ 24hrs. The resolution of the System is 2.1 FWHM, a peak to Compton ratio of 26:1 and a counting absolute photopeak efficiency of 5.5%, all compared at 1332 KeV photopeak of Co-60. The spectral data were stored on magnetic tapes which were subsequently processed using the Compute program "SAMPO" on the University of London computers. The final output are tables of results giving computed photopeak energies, channel locations, peak areas with corresponding estimated uncertainties. Optional output from the program includes peak areas corrected for decay and dead-time, gamma-ray abundance, relative intensity and the ratio of peak area to detection efficiency with their uncertainties. In this work, however the peak areas of interest were corrected for decay and dead-time manually. The assignment of isotopes to the observed peaks was also carried out

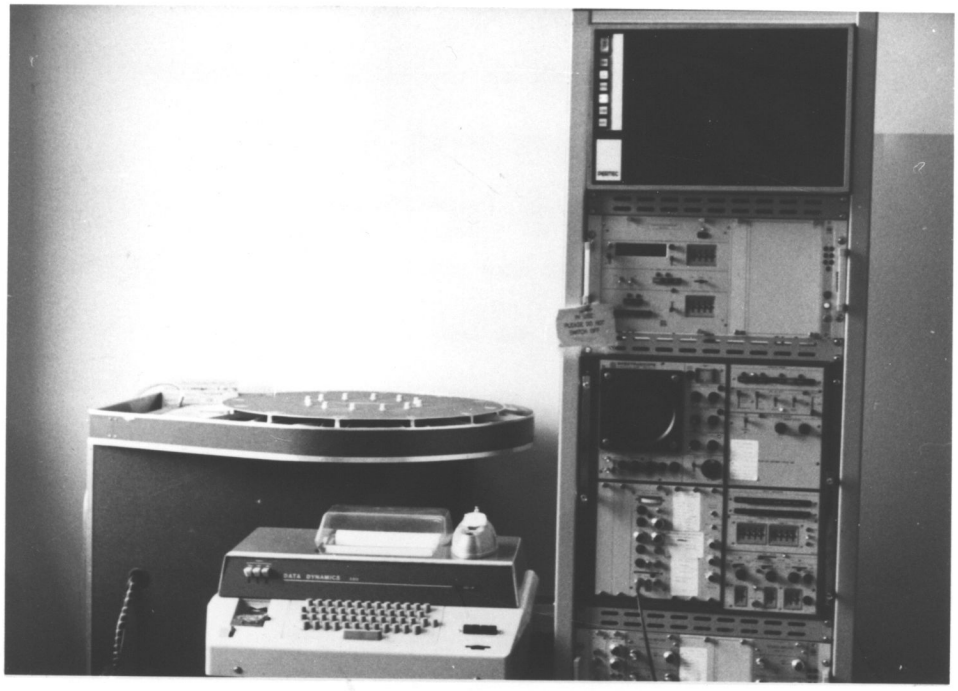

Figure 7.3 Counting equipment showing the Ge(Li) detector coupled to 4096 MCA Laben 8000 system with the Magnetic Tape interface and the Teletype.

manually, using the energies, branching ratios (in intensities of gamma-rays) of associated peaks and half-life obtained from the IDENT. Compilation (23). Additional data were obtained from the Table of Isotopes (24) and the Nuclear Data Tables (25).

(1) Qualitative results

The program "SAMPO" was used to search all spectra for statistically significant peaks (PEAKFIND algorithm) using the minimum search significance criteria (3) of 2 permanently stored in the program. This level of significance was chosen so that many peaks, particularly the less intense in the lower energy region could be included in the output. An output with peak energies, channel locations and the associated peak significance for all peaks found was obtained for each spectrum. This was then carefully inspected, and on the basis of data in the Nuclear Data Library (23) which gives the energy, isotope, gamma-ray intensity, most intense gamma-ray of the isotope, half-life, cross section and natural abundance of the isotope, a preliminary assignment of isotopes to the peaks found in the spectrum was carried out. Using additional information about the elemental composition of the materials as certified by the Suppliers, isotopes contributing to the observed peaks were finally assigned. In tables 3, 4 and 5 are presented the results of the elements detected via Instrumental Neutron Activation Analysis applying the three modes (i.e. A, B and C) of irradiation and counting, respectively. The tables give the elements and the corresponding product isotopes, the half-life of the isotopes and the gamma-ray energies observed. In cases where an isotope emits more than one gamma-ray, all energies are reported if they were observed. In the biological standard Reference Materials i.e. NBS 1577 (Bovine Liver), NBS 1571 (Orchard Leaves), Bowen's Kale (27), Animal Muscle (IAEA) (28) and Animal Blood (IAEA), 20 elements were detected under the 60 seconds irradiation (mode A). The majority of these elements were,

MODE A TABLE 3.

ISOTOPE	$T_{\frac{1}{2}}$	Eγ (KeV)	ANIMAL MUSCLE	ANIMAL BLOOD	BOVINE LIVER	BOWENS KALE	ORCHARD LEAVES	ARGILLACEOUS LIMESTO
^{85m}Sr	1.17hr	231.5	-	-	-	-	-	✓
^{117m}In	1.9 hr	315.2	✓	-	-	-	-	-
^{51}Ti	5.78min	320.	-	-	-	-	-	✓
^{87m}Sr	2.83hr	388.5	-	-	-	✓	-	-
^{126}I	25.3min	442.7	-	✓	-	-	-	-
^{86m}Rb	1.04min	555.8	-	-	-	✓	-	-
^{80}Br	17.6 min	617.0	✓	✓	✓	✓	✓	✓
^{27}Mg	9.5 min	844.0	✓	✓	✓	✓	-	✓
^{56}Mn	2.58hr	846.9	-	✓	✓	✓	✓	-
^{51}Ti	5.8 min	928.5	✓	-	-	-	-	-
^{152m}Eu	9.3 hr	963.5	-	-	-	-	-	-
^{27}Mg	9.5 min	1014.1	✓	✓	✓	✓	✓	✓
^{66}Cu	5.1 min	1040.	-	✓	✓	-	✓	-
^{116m}In	54min	1097.1	-	-	-	-	-	✓
^{31}Si	2.6 hr	1266.2	-	-	-	-	-	✓
^{24}Na	15.0 hr	1368.4	✓	✓	✓	✓	✓	✓
^{52}V	3.75min	1434.4	-	✓	✓	✓	✓	✓
^{42}K	12.4 hr	1524.7	✓	✓	✓	✓	✓	✓
^{38}Cl	37.2 min	1642.	✓	✓	✓	✓	✓	✓
^{28}Al	2.31min	1778.9	✓	-	✓	✓	✓	✓
^{56}Mn	2.58hr	1810.9	-	✓	✓	✓	✓	-
-	-	2112.8	-	✓	✓	✓	✓	-
^{38}Cl	37.2min	2166.8	✓	✓	✓	✓	✓	✓
^{24}Na	15.0hr	2753.6	✓	✓	✓	✓	✓	✓
^{49}Ca	8.7min	3083.	✓	✓	✓	✓	✓	✓
^{37}S	5.1min	3102.4	-	-	✓	✓	✓	-
^{49}Ca	8.7min	4073.0	✓	✓	✓	✓	✓	✓

MODE B TABLE 4

ISOTOPE	$T_{\frac{1}{2}}$	E_γ (KeV)	ANIMAL MUSCLE	ANIMAL BLOOD	BOVINE LIVER	BOWENS KALE	ORCHARD LEAVES	ARGILLACEOUS LIMESTO
^{171}Er	7.53hr	124.	-	-	-	-	-	-
^{139}Ba	1.41hr	165.8	-	-	-	-	-	-
^{27}Mg	9.5min	171.0	✓	-	-	-	-	-
^{85m}Sr	1.17hr	231.5	-	-	-	-	-	-
^{42}K	12.4hr	312.9	✓	-	✓	-	✓	-
^{51}Ti	5.78min	320.0	✓	-	-	-	-	-
^{180m}Hf	5.5min	332.2	-	-	-	-	-	-
^{117}Cd	2.73hr	345.0	-	-	-	-	-	-
^{159}Gd	18.6 hr	363.6	-	-	-	-	-	-
^{87m}Sr	2.83hr	388.5	-	-	✓	✓	✓	✓
^{86m}Rb	1.04min	555.8	-	-	-	✓	-	-
^{51}Ti	5.78min	575.0	✓	-	-	-	-	-
^{80}Br	17.6 min	617.0	✓	✓	✓	✓	✓	✓
-	-	665.7	-	-	✓	-	-	✓
-	-	704.3	-	-	✓	-	-	-
^{165}Dy	2.33hr	715.3	-	-	-	-	-	-
^{82}Br	35.8 hr	776.8	-	-	-	-	✓	-
^{72}Ga	14.1 hr	834.0	-	-	-	-	-	-
^{27}Mg	9.5min	844.0	✓	✓	-	✓	-	✓
^{152m}Eu	9.3 hr	963.5	-	-	-	-	-	-
^{116m}In	54 min	1097.1	-	-	-	-	-	✓
^{27}Mg	9.5min	1014.1	✓	✓	✓	✓	✓	✓
^{66}Cu	5.1min	1040.	-	-	-	-	✓	-
^{31}Si	2.6 hr	1266.2	-	-	-	-	-	-
^{29}Al	6.6min	1273.3	-	-	-	-	-	-
^{116m}In	54 min	1293.4	-	-	-	-	-	✓
^{24}Na	15.0hr	1368.4	✓	✓	✓	✓	✓	✓
^{52}V	3.75min	1434.4	✓	-	-	✓	✓	✓
^{42}K	12.4 hr	1524.7	✓	✓	✓	✓	✓	✓
^{38}Cl	37.2 min	1642.0	✓	✓	✓	✓	✓	✓
^{28}Al	2.31min	1778.9	✓	✓	✓	✓	✓	✓
^{56}Mn	2.58hr	1810.9	-	-	✓	-	✓	-
^{38}Cl	37.2min	2166.8	✓	✓	✓	✓	✓	✓
^{24}Na	15.0 hr	2753.6	✓	✓	✓	✓	✓	-
^{49}Ca	8.7min	3083.	✓	✓	✓	✓	✓	✓
^{37}S	5.1min	3102.4	-	✓	-	-	-	-
^{49}Ca	8.7min	4073.0	✓	✓	✓	✓	✓	✓

MODE C TABLE 5

ISOTOPE	$T_{\frac{1}{2}}$	Eγ (KeV)	ANIMAL MUSCLE	ANIMAL BLOOD	BOVINE LIVER	BOWEN'S KALE	ORCHARD LEAVES	ARGIL CEOU LIMES
^{42}K	12.4hr	312.9	-	-	✓	✓	-	-
^{51}Ti	5.78min	320.0	-	-	-	-	-	-
^{87m}Sr	2.83hr	388.5	-	-	✓	✓	-	-
^{116m}In	54min	417.0	-	✓	-	-	-	-
^{128}I	25.3min	442.7	-	✓	-	-	✓	-
-	-	526.3	-	-	-	-	✓	-
^{80}Br	17.6min	617.0	✓	✓	✓	✓	✓	✓
^{81}Se	18min	649.3	-	-	-	-	✓	-
^{80}Br	17.6min	665.7	✓	✓	✓	✓	✓	✓
^{82}Br	35.8hr	776.6	-	-	-	✓	-	-
^{27}Mg	9.5min	844.0	✓	-	✓	-	-	-
^{56}Mn	2.58hr	846.9	-	✓	✓	✓	✓	✓
^{27}Mg	9.5min	1014.1	✓	-	✓	✓	-	✓
^{116m}In	54min	1097.1	-	-	-	-	-	✓
-	-	1293.4	-	✓	-	-	-	✓
^{24}Na	15.0hr	1368.4	✓	✓	✓	✓	✓	✓
^{52}V	3.75min	1434.4	✓	✓	-	-	-	✓
^{42}K	12.4hr	1524.7	✓	-	✓	✓	✓	✓
^{38}Cl	37.2min	1642.0	✓	✓	✓	✓	✓	✓
^{28}Al	2.31min	1778.9	✓	-	✓	✓	✓	✓
^{56}Mn	2.58hr	1810.9	-	✓	✓	✓	-	✓
-	-	2112.8	-	✓	✓	-	-	✓
^{38}Cl	37.2min	2166.8	✓	✓	✓	✓	✓	✓
^{24}Na	15.0hr	2753.6	✓	✓	✓	✓	✓	✓
^{49}Ca	8.7min	3083	✓	-	✓	✓	✓	✓
^{37}S	5.1min	3102.4	-	-	-	-	✓	-
^{49}Ca	8.7min	4073	✓	-	✓	✓	✓	✓

however found to be present in all cases. Thus ^{80}Br (T = 17.6 min), ^{24}Na(T = 15.0 hr), ^{28}Al(T = 2.31 min), ^{38}Cl(T = 37.2 min), ^{27}Mg(T = 9 ^{42}K(T = 12.4 hr) and ^{49}Ca(T = 8.7 min) were easily detected in all sa The ^{56}Mn(T = 2.58 hr) isotope was present in the other four materials could not be seen in Animal Muscle (IAEA). This suggests, probably low concentration of the element in Animal Muscle. Three metastable isotopes, ^{117m} In(T = 1.9 hr) in Animal Muscle, ^{87m} Sr(T = 2.83 hr) ar ^{86m} Rb(T = 1.04 min) in Bowen's Kale were also detected. Copper (^{66}Cu T = 5.1 min) and Sulphur (T = 5.1 min) were both detected in Orchard L Bovine Liver with Sulphur also found in Bowen's Kale as well, Vana (^{52}V, T = 3.75 min) was easily identified in Animal Blood, Bovine Live and Bowen's Kale. ^{128}I(T = 25.3 min) was, however only seen in Anima Blood. At least 6 of the most common elements present in the biologi Standards were found in the two Geological materials as well. In addi ^{152m}Eu(T = 9.3 hr) ^{116m}In(T = 54 min) and ^{31}Si(T = 2.6 hr) gave rise t detectable activities in NBS 1c (Argillaceous Limestone). In all sam it was noted that the greater part of the Ge(Li) counting rate was cont buted by the above listed common radionuclides; namely ^{24}Na, ^{80}Br, ^{42}K, ^{27}Mg, ^{28}Al, ^{56}Mn, ^{38}Cl, and ^{49}Ca.

Table 4 shows the isotopes corresponding to elements detected u conditions under mode B. In all 21 elements with neutron product isot were observed. Of these, the largest contribution of new elements dif from those seen under mode A comes from the Geological materials, and i particular NBS97C (Flint Clay). Among the new elements found in Flint were ^{171}Er(T = 7.53 hr), ^{139}Ba(T = 1.41 hr), ^{117}Cd(T = 2.42 hr), ^{159}Gd(18.6 hr), ^{180m}Hf(T = 5.5 min), ^{165}Dy(T = 2.33 hr), and ^{72}Ga(T = 14.1 hr Essentially, the same elements found in mode A were found in mode B for biological materials. It is clear from the table that most of the ele detected are those whose neutron product isotopes are low-energy gamma-r

emitters. Uncertainties (due to manual identification) as to the presence of these isotopes here is expected, since as is always the c Compton scattering from the higher energy gamma-rays presents a major problem in this part of the energy spectrum. These results are an average of at least three spectra per sample. So that it was only a the peak had been observed in all three spectra that it was assigned isotope. Finally, table 5 shows the isotopes determined using condi in mode C. Again the isotopes ^{24}Na, ^{27}Mg, ^{56}Mn, ^{38}Cl, ^{42}K, ^{28}Al, ^{80} ^{49}Ca and ^{37}S (to a lesser extent) are present in all materials. Basic the same number of isotopes as found in mode B are also found in mode However, the major difference between these two modes is that low ener gamma-rays have become less significant in mode C. This phenomenon w seem to suggest an interference arising from the build-up in activity the longer-lived and higher energy gamma-emitting isotopes masking the intense low energy gamma-rays. Perhaps the best example of this effe seen between ^{56}Mn(T = 2.58 hr) and ^{27}Mg(T = 9.5 min) in Bowen's Kale. mode B ^{56}Mn is seen at 846.9 KeV and ^{27}Mg is identified at 844.0 KeV well as 1014.1 KeV peak. However in mode C ^{27}Mg can only be identifi through one peak at the less intense but interference-free higher ener gamma-ray at 1014.1 KeV since it is clear that ^{56}Mn at 846.9 KeV overc and floods the signal from ^{27}Mg and the two cannot be resolved.

For routine instrumental neutron activation based on the compa method, the use of these Standard Reference Materials should prove reas reliable in the assay of short-lived isotopes. Manual assignment of t activation products using the documented nuclear properties of the isot will not, however, always produce positive identification of the specie contributing to the observed peaks in the spectrum. For elements with large activation cross sections, the identification on a routine basis fairly simple, particularly if they have short-lived isotopes. In case

where an isotope emits two gamma-rays of relatively equal intensity (e ^{24}Na, 1368.4 I = 47 and 2753.6 I = 52) the two gamma-ray energies are well separated thus strengthening the evidence for the presence of the element of interest.

(2) Quantitative results

All elemental mass concentrations were calculated using the pe areas computed by the program "SAMPO" treating NBS 1571 (Orchard Leave and NBS 1C (Argillaceous Limestone) as the irradiation standards for B logical and Geological Reference Materials respectively. Orchard Leav was chosen for its wide range of certified elements (at least 25 elemer and Argillaceous Limestone gave the best representative elemental compo tion of geological materials. An example of the table of results givi peak areas corresponding to the statistically acceptable peaks is shown table 6. All the areas were first corrected for decay, and dead-time effects before converting them into elemental mass. To minimize the e arising from differences in weight of the samples, peak areas were divi by the corresponding mass of the sample, thus giving the area in counts unit mass. Peak areas for quantitation were selected on the basis of s ful identification of the contributing isotopes to the observed peaks a the severity of interference from neighbouring peaks. Thus, in the pre of ^{56}Mn, ^{27}Mg was measured using the peak area at 1014.1 KeV instead of more intense 844.0 KeV gamma-ray because of the obvious contribution fro ^{56}Mn 846.9 KeV gamma-ray. Similarly, ^{56}Mn in high concentration levels ^{27}Mg had to be quantified through the 1810.7 KeV or 2112.8 KeV for which there is minimum interference in the neighbourhood. The degree of inte ference between neighbouring peaks is mainly determined by the resolutio the detector in the energy range of the peaks. Peaks were considered n to interfere with each other if they were separated by at least a minimu

RUN NUMBER AND INDICATIVE DATA
OPERATED LEAVES 3 UL9359
COMMENTS =

0 0 4100
DATE = 03/03/78

ENERGIES RECOMPUTED USING OPTION 2

AREA COUNTS CORRECTED FOR DEAD TIME / UNIT MASS WAITING TIME 735.00SECS SAMPLE WEIGHT 230.0 MG LIVE TIME 589.9CLOCKTIME 600.0

TABLE OF RESULTS

NUMBER	CHANNEL	CHANNEL ERROR	ENERGY IN KEV	ENERGY ERROR	AREA COUNTS	PC-AREA ERROR	POSSIBLE ISOTOPE		ACTUAL ENG.KEV	MICRO G/G	T ERROR PC	TM CORR AREA
1	52.560	.493	51.382	.596	.683E+01	22.73						
2	76.012	.162	74.851	.526	.124E+01	15.48	PbXRAY		74.70			.122E+01
3	86.261	.195	85.108	.537	.113E+01	18.55						
4	321.051	.100	320.069	.510	.121E+01	9.42	CR51		320.00			
5	511.747	.063	510.903	.504	.456E+01	4.29	ANHIL		511.00			.121E+01
6	617.690	.065	616.923	.504	.215E+01	5.89	BR82		616.00			.456E+01
7	789.393	.100	788.751	.510	.710E+00	8.73	MN56DE		788.00			.215E+01
8	847.370	.002	846.770	.500	.556E+02	3.50	MN56		847.00			.756E+00
9	1015.053	.038	1014.514	.501	.287E+01	3.49	MG27		1014.00			.692E+02
10	1091.499	.117	1090.988	.514	.521E+00	10.05	MN56DE		1091.00			.706E+01
11	1145.463	.155	1144.972	.523	.709E+00	10.19	CL38 DE		1145.00			.656E+00
12	1294.134	.145	1293.715	.521	.543E+00	13.04	FE59		1292.00			.890E+00
13	1369.183	.003	1368.773	.500	.592E+00	7.56	NA24		1368.00			.543E+00
14	1525.225	.001	1524.715	.500	.251E+01	3.49	K42		1525.00			.900E+00
15	1643.162	.039	1642.583	.502	.321E+01	3.23	CL38		1642.00			.254E+01
16	1779.335	.002	1779.055	.500	.138E+01	5.20	AL28		1779.00			.403E+01
17	1811.189	.024	1810.979	.501	.803E+01	1.91	MN56		1811.00			.538E+02
18	2062.750	.003	2062.550	.500	.151E+01	4.31	CA49	DE	2061.00			.848E+01
19	2113.508	.033	2113.583	.501	.351E+01	2.50	MN56		2113.00			.396E+01
20	2167.684	.048	2167.903	.502	.316E+01	3.19	CL38		2157.00			.371E+01
21	2573.131	.005	2573.109	.500	.705E+00	7.05	CA49	SE	2572.00			.399E+01
22	3043.985	.085	3043.527	.508	.215E+01	5.32	CA49		3043.00			.185E+01
												.568E+01

Table 6 Typical Table of Results Obtained from the Analysis Routine.

twice the resolution of the system at FWHM (i.e. at least 6 channels). Out of the total number of elements indicated present in the Standard Reference Materials analyzed, as shown in the qualitative results in Section 4.1(1), 9 isotopes were found suitable for quantitative determination. These are ^{80}Br, ^{28}Al, ^{42}K, ^{38}Cl, ^{27}Mg, ^{24}Na, ^{49}Ca, ^{66}Cu and ^{56}Mn. It should be mentioned that some of these elements are not at trace levels in some Standard Reference Materials, e.g. Potassium and Calcium are major constituents in Orchard Leaves. Nevertheless, quantification was found necessary in order to obtain the best precision and accuracy and hence demonstrate the usefulness of short-lived elemental assay. The results of the 11 elements found under the three modes i.e. A, B, C of irradiation, delay and counting conditions are given in tables 7.1, 7.2, 7.3 and 7.4 for biological materials and table 8 for the geological SRM's. The results of the elemental concentration found in this work are presented in parts per million (ppm) or percentage by weight (% wt) along with those values reported in literature where they were available. The figures enclosed in brackets represent the estimates of the spread in the value either in standard deviation or range. In this work, the standard deviation of the elemental mass concentrations calculated was determined using the following equation :

$$\left(\frac{\delta m_x}{m_x}\right)^2 = \left| \left(\frac{\delta A_{cx}}{A_{cx}}\right)^2 + \left(\frac{\delta A_{cs}}{A_{cs}}\right)^2 + \left(\frac{\delta m_s}{m_s}\right)^2 \right|^2 \qquad (25)$$

where, δm_x - uncertainty in the mass of the element determined in the sample,

δA_{cx} - uncertainty in the corrected number of counts (area) due to the element in the sample,

δA_{cs} - uncertainty in the corrected number of counts (area) due to the same element in the Standard,

δm_s - uncertainty in the mass of the element in the Standard.

Table 7.1

NBS 1577 Bovine Liver

Element	Isotope	Half-life	Gamma-ray used for quantitation (KeV)	Mode A ppm/%wt	Mode B ppm/%wt	Mode C ppm/%wt	Literature Value ppm/%wt
Aluminium	^{28}Al	2.31min	1778.9	30.5(6)	38.4(3)	40.6(4)	45.6(2.7)
Bromine	^{80}Br	17.6min	617.0	12.8(2)	8.9(.5)	10.2(1.5)	9.59
Potassium	^{42}K	12.4hr	1524.7	7800(140)	9400(120)	8600(150)	9700
Chlorine	^{38}Cl	37.2min	1642.0	4500(130)	3000(75)	2850(100)	2660
Magnesium	^{27}Mg	9.5min	1014.1	1200(68)	880(48)	1000(50)	610
Manganese	^{56}Mn	2.58hr	846.9	20.5(2)	8.9(1.4)	14.2(2)	10.3
Sodium	^{24}Na	15.0hr	1368.4	1960(70)	2000(106)	3400(120)	2400(100)
Calcium	^{49}Ca	8.7min	3083.0	80.6(24)	160(14.6)	102(20)	124.0
Copper	^{66}Cu	5.1min	1040.0	-	-	150(26)	193.0

Table 7.2

Bowen's Standard Kale

Element	Isotope	Half-life	Gamma-ray used for quantitation (KeV)	Mode A ppm/%wt	Mode B ppm/%wt	Mode C ppm/%wt	Literature Value ppm/%wt
Aluminium	$^{28}A\ell$	2.31min	1778.9	24.6(3)	48.2(4.2)	42(5)	38.2(6.4-88.4)
Bromine	^{80}Br	17.6min	617.0	32.8(2.1)	25.8(1.2)	28.4(1.5)	26.1
Potassium	^{42}K	12.4hr	1524.7	19720(200)	21900(230)	23000(200)	24615
Chlorine	$^{38}C\ell$	37.2min	1642.0	2840(315)	4660(400)	4850(420)	3415(2180-4450)
Magnesium	^{27}Mg	9.5min	1014.1	2010(214)	1780(200)	1420(160)	1572(1350-1700)
Manganese	^{56}Mn	2.58hr	846.9	23.6(5)	15.2(3.9)	18.6(3)	14.73(12.6-18)
Sodium	^{24}Na	15.0hr	1368.4	3450(360)	2330(300)	2430(420)	2506(1220-3250)
Calcium	^{49}Ca	8.7min	3083.0	28800(900)	42107(1213)	38670(1022)	40850

Table 7.3

IAEA ANIMAL BLOOD

Element	Isotope	Half-life	Gamma-ray used for quantitation (KeV)	Mode A ppm/%wt	Mode B ppm/%wt	Mode C ppm/%wt	Literature Valu ppm/%wt
Aluminium	$^{28}A\ell$	2.31min	1778.9	102(25)	70.32(12)	80.6(14)	N.A.
Bromine	^{80}Br	17.6min	617.0	30.1(6)%	8.61(1.8)%	10.2(2)%	-
Potassium	^{42}K	12.4hr	1524.7	10.3(1)%	4.0(.02)%	5.8(.7)%	-
Chlorine	$^{38}C\ell$	37.2min	1642.0	1204(45)	1625.76(22)	1450(18)	-
Sodium	^{24}Na	15.0hr	1368.4	425(20)	326.76(6.3)	400(11)	-
Magnesium	^{27}Mg	9.5min	1014.1	9.2(2)	3.88(.2)%	4.52(1)	-

N.A. Not available

Table 7.4 IAEA ANIMAL MUSCLE

Element	Isotope	Half-life	Gamma-ray used for quantitation (KeV)	Mode A ppm/%wt	Mode B ppm/%wt	Mode C ppm/%wt	Literature Value ppm/%wt
Aluminium	$^{28}A\ell$	2.31min	1778.9	12.4(2)	9.9(1.5)	12.3(4)	N.A.
Bromine	^{80}Br	17.6min	617.0	2.5(1.0)	3.5(1)	5.2(.8)	-
Potassium	^{42}K	12.4hr	1524.7	11400(150)	14500(120)	13800(310)	-
Chlorine	$^{38}C\ell$	37.2min	1642.0	2000(50)	1860(40)	1920(40)	-
Magnesium	^{27}Mg	9.5min	1014.1	980(40)	1020(30)	1100(30)	-
Sodium	^{24}Na	15.0hr	1368.4	2030(60)	2090(70)	2110(80)	-

N.A. - Not available

(3) Precision and accuracy

Since this exercise involved using Standard Reference Materials both as analytical samples and irradiation standards, many of which are well characterised, precision and accuracy of the results obtained was estimated by comparing the calculated values with literature values where they were available. In the absence of literature values, a weighted mean of the computed values was used. Applying this definition in the three modes for both biological and geological materials, it can be seen that there is a general lack of agreement between the calculated values and those reported in literature in mode A. The results obtained in mode B show a much better agreement, whereas those in mode C are slightly better than those in mode A, but no better than mode B in this respect. The average coefficient of variation in the determinations was estimated to be between 15% and 30% in mode A, 3% and 20% in mode B and between 10% and 40% in mode C. The best overall precision was obtained in the results in mode B for all the Reference Materials. In general, the largest deviations were observed in the values for ^{24}Na, ^{38}Cl, ^{42}K and to a lesser extent in ^{49}Ca. The elevation in the values for these isotopes is most unlikely due to external contamination during sample preparation. In the case of ^{24}Na, it is also possible that there was a significant contribution from the $^{27}Al(n,\alpha)\ ^{24}Na$ reaction in materials with high levels of Aluminium. The magnitude of this contribution was not, however estimated in this part of the experiment. In all the results, better agreement between calculated values and literature values was indicated by elemental mass determinations of ^{80}Br and ^{56}Mn in all modes. An average deviation of 4% representing a factor of 2 lower and 4 upper than the reported values of these elements was observed in the majority of the determined values. The values for ^{28}Al do not deviate very significantly in most determinations, which would seem to indicate a reduced contribution from the $^{31}P(n,\alpha)\ ^{28}Al$ reaction. Most of

the observed variations can be attributed to the irradiation conditions an measurements of the activities. More importantly in this respect, is the effect of dead-time when counting short-lived activities, particularly in mode A. Also significant in this respect is the problem of huge Compton background activities from the high energy gamma-rays of short-lived isotopes which quickly overcome and mask the low energy peaks. Typical in this case is the ^{66}Cu at 1040 KeV in Bovine Liver which could not be detected in mode A and B mainly because of the Compton edge due to 1368.4 KeV ^{24}Na. The failure in the values obtained in mode C to agree closely with the literature can be attributed to errors arising from the matrix activity interference. Since even irradiations of 20 minutes long in a flux of 10^{12} n cm^{-2} s^{-1} would produce significant long-lived activities in nuclides with favourable activation properties which are in abundance in the samples such as ^{23}Na, ^{41}K and ^{37}Cl.

The main factors believed to be responsible for the measured precision and accuracy in this experiment are :

(1) Self-shielding of the samples and the standard due to different sizes and concentrations,

(2) Sample inhomogeneity (to a much lesser extent),

(3) Variation of the neutron flux at different positions of the samples,

(4) Non-reproducibility of the detector-source geometry.

(5) Statistical variations in the counting.

Effects from the last factor were minimized by choosing a constant time of counting.

Although the overall determinations in all the three modes are not particularly accurate, it is important to note that most of the values

determined are within a useful range for most general applications in Instrumental Neutron Activation Analysis where usually the knowledge of the order of magnitude of the elemental content is sufficient.

(4) Detection limits for mode B

It was considered useful to calculate detection limits for the elements detected using the irradiation, delay and counting scheme developed in mode B, since mode B provided the best optimum detection conditions for quantitative determinations. The detection limits for all the elements detected (see table **9**) are based on the criteria $S \geq \sqrt{B}$ in this matrix (20), B being the matrix background activity. The baseline under the fitted peak using "SAMPO" (usually 11-20 channels) was summed and used in obtaining the values given in table **9**. The values agree reasonably well with those found in literature within experimental errors.

(5) Discussion

In general the application of short-lived radionuclides in neutron activation analysis offers a number of advantages compared to the use of long-lived radionuclides. The most important factor is that of economy. It is obvious that a short activation time in a nuclear reactor is desirable in terms of economy, and more so in accelerators where long activation times are impractical, mainly because of the limited lifetime of the target producing neutrons. The other consideration in favour of short activation times is the capability to produce results rapidly after sampling, enabling one to carry out a large number of analyses on a routine basis. The usefulness of any short-lived activation however, has to be evaluated in terms of sensitivity and liability to interferences with respect to the matrix in question. In practice the choice of a short-lived radionuclide is one of the determining factors in the selection of optimum detection conditions. In the final analysis, the

Table 9 DETECTION LIMITS FOR MODE B:BOWEN'S KALE 240mg

Element	Reaction	$T_{\frac{1}{2}}$	Selected γ-ray (KeV)	$2\sqrt{B}$	Detection limit ppm
Aluminium	$^{27}A\ell(n,\gamma)^{28}A\ell$	2.31min	1778.9	503	9
Bromine	$^{79}Br(n,\gamma)^{80}Br$	17.6min	617.0	596.6	1.4
Potassium	$^{41}K(n,\gamma)^{42}K$	12.4hr	1524.7	414.2	902
Chlorine	$^{37}C\ell(n,\gamma)^{38}C\ell$	37.2min	1642.0	537.1	36
Magnesium	$^{26}Mg(n,\gamma)^{27}Mg$	9.5min	1014.1	667.4	377.5
Manganese	$^{55}Mn(n,\gamma)^{56}Mn$	2.58hr	846.9	386.9	0.24
Copper	$^{65}Cu(n,\gamma)^{66}Cu$	5.1min	1040.0	480	6.8
Sodium	$^{23}Na(n,\gamma)^{24}Na$	15.0hr	1368.4	653.4	33
Calcium	$^{48}Ca(n,\gamma)^{49}Ca$	8.7min	3083.0	156.3	313

overriding principle in any method adopted is the type and nature of the analytical goals. In analyses of an exploratory nature it may only be required to obtain qualitative information indicating the presence or absence of certain elements. In other experiments, particularly in routine applications the content of an element in a given matrix may be important at any level so that errors of ± 10 - 20% such as encountered in modes A and C are acceptable. In such cases, the shortest irradiations possible (mode A) would seem to be suitable. However, in other applications in particular trace-element research where accurate determination of elemental concentration in materials is crucial, it is the method giving the best precision and accuracy which is always preferred, however time consuming or expensive it may be.

4.2 Epicadmium irradiations

Three of the Standard Reference Materials were subject to irradiation and counting conditions developed in mode B under Cadmium Cover, in an attempt to investigate the usefulness of epithermal activation. NBS 1571 (Bovine Liver), Bowen's standard Kale and NBS 1577 (Orchard Leaves) were chosen as test materials for this exercise. Respective spectra were collected on magnetic tapes and processed as before using "SAMPO". The peak areas corresponding to radioisotopes analyzed in 4.1.1 were obtained. These were divided by the mass of the sample in each case giving the area in counts per unit mass. Another set of these materials was also irradiated in a mixed reactor flux as in 4.1.1 and treated identically. The results of the experiment are given in table 11. In the table, the element and the corresponding radioisotope, the gamma-ray considered (as in 4.1.1), and the corrected peak areas with the associated errors as obtained from the program "SAMPO" for both mixed flux and epithermal irradiation are given. The

Table 11.1

NBS 1577 (Bovine Liver)

I_{act} = Resonance activation integral, B = Background under the Peak

Element	Isotope	Mixed flux irradiation, sample mass = 233.5mg					Epicadmium irradiation, sample mass = 217.77mg				
		Selected γ-ray(KeV)	Peak area	Error %	B	area/mass	Peak area	Error %	B	area/mass	I_{act}(barns)
Aluminium	$^{28}A\ell$	1778.9	25700	.84	24972	110	14100	1.43	38541	64.76	.18
Bromine	^{80}Br	617.0	12200	1.4	48966	52.2	42600	.67	69642	195.68	153
Sodium	^{24}Na	1368.4	18000	.78	48708	77.1	18500	1.28	66994	84.9	.29
Potassium	^{42}K	1524.7	1970	3.3	53826	8.4	5930	1.47	52600	27.2	.96
Manganese	^{56}Mn	846.9	14100	1.1	39735	60.4	26600	1.28	46406	122.2	14
Magnesium	^{27}Mg	844.0 1014.1	-	-	-	-	1910	4.14	64281	8.8	-
Copper	^{66}Cu	1040.0	3160	2.5	61532	13.5	499	16.5	38496	2.3	2.6
Chlorine	$^{38}C\ell$	1642	12100	1.04	12807	51.8	18500	1.1	24383	84.9	14
Calcium	^{49}Ca	3083	-	-	-	-	7150	1.68	4182	32.8	-

Table 11.2

BOWEN'S KALE

I_{act} = Resonance activation integral,

B = Background under the Peak

		Mixed flux irradiation, sample mass = 603.2mg					Epicadmium irradiation, sample mass = 304.4mg				
Element	Isotope	Selected γ-ray(KeV)	Peak area	Error %	B	area/mass	Peak area	Error %	B	area/mass	I_{act}(barns)
Aluminium	$^{28}A\ell$	1778.9	2050	4.6	63252	3.39	24700	1.74	23844	81.4	.18
Bromine	^{80}Br	617.0	9760	3.4	88983	16.2	11400	1.8	45573	37.45	153
Sodium	^{24}Na	1368.4	50000	1.6	106733	82.89	16900	.71	46746	55.5	.29
Potassium	^{42}K	1524.7	11300	1.6	42890	18.7	1740	4.1	41140	5.7	.96
Manganese	^{56}Mn	846.9	36300	2.9	111355	60.2	13200	1.2	34878	43.4	14
Magnesium	^{27}Mg	844.0 1014.1	2930	1.9	37423	4.86	1390	3.4	78510	4.5	-
Copper	^{66}Cu	1040	-	-	-	-	3170	2.1	58817	10.4	2.6
Chlorine	$^{38}C\ell$	1642	50200	1.4	72119	83.2	11300	.84	29006	37.1	14
Calcium	^{49}Ca	3083	20500	.9	61074	33.98	-	-	-	-	-

Table 11.3 NBS 1571 (Orchard Leaves)

		Mixed flux irradiation, sample mass = 175.2mg					Epicadmium irradiation, sample mass = 248.7mg				
Element	Isotope	Selected γ-ray(KeV)	Peak area	Error %	B	area/mass	Peak area	Error %	B	area/mass	I_{act}(barns)
Aluminium	$^{28}A\ell$	1778.9	1964	5.7	69451	11.21	29800	.75	19049	119.8	.18
Bromine	^{80}Br	617.0	3497	6.2	143919	19.9	12200	1.2	87285	49.1	153
Sodium	^{24}Na	1368.4	94518	1.8	113626	539.5	1880	4.0	40541	7.55	.29
Potassium	^{42}K	1524.7	2139	5.5	83749	12.2	3220	2.5	44167	12.9	.96
Manganese	^{56}Mn	846.9	214194	2.3	95651	1222.57	13900	3.0	38851	55.9	14
Magnesium	^{27}Mg	1014.1	-	-	-	-	7500	1.3	47178	30.2	-
Copper	^{66}Cu	1040.0	-	-	-	-	9320	3.5	8432	37.5	2.6
Chlorine	$^{38}C\ell$	1642.0	66897	.6	79272	382	2980	2.4	24739	11.98	14
Calcium	^{49}Ca	3083	1272	3.8	3999	7.26	322	2.2	1145	1.29	-

background underlying the peak in all cases was obtained by summing the channels (usually 11 channels for $E_\gamma \leq 1.2$ MeV and 20 channels for $E_\gamma \leq 1.2$ MeV) spanning the baseline under the fitted peak. Also included in the table are values of resonance activation integrals for the isotopes considered where they were available.

The irradiations were performed in the ICIS facility of the University of London Reactor Centre as in 4.1.1. The thermal flux in this position is 1.7 $x10^{12}$n.cm^{-2} s^{-1} and the fast flux is 8.58 x 10^{11}n.cm^{-2} s^{-1} with a Cadmium Ratio (R_{Cd}) for Au of 2.33. The main aim in this exercise was to irradiate the three Reference Materials (i.e. Bovine Liver, Orchard Leaves and Bowen's Kale) under Cadmium cover (i.e. epithermal activation) and collect respective gamma-ray spectra; and compare the results with those obtained for the same materials in the mixed flux irradiation. This was considered useful in that some basic features characterizing the two activation techniques would be identified, particularly with respect to biological materials.

From the tables (table 11.1, 11.2, 11.3), it can be seen that in general the background spectra are greatly reduced in the case of epithermal activation when compared with mixed flux activation. This certainly is an important advantage for epithermal activation when compared with mixed flux activation. This certainly is an important advantage for epithermal activation as it means that large values of signal-to-noise ratios can be obtained leading to high detection sensitivities for the elements of interest. In mixed flux neutron activation, this is not easily achieved and the signal-to-noise ratio can only be enhanced with the use of specialized techniques such as the cyclic activation method (see 1.2). Tables 12.1, 12.2 and 12.3 show experimental values of signal-to-noise ratios due to the gamma-rays measured in both mixed and epithermal activation for the three Reference

Table 12.1 NBS 1577 (Bovine Liver)

Isotopes	Gamma-ray energy (KeV)	Mixed			Epithermal			Epithermal/Mixed
		S	$\sqrt{B}$	$R_{SN}=S/\sqrt{B}$	S	$\sqrt{B}$	$R_{SN}=S/\sqrt{B}$	$(R_{SN})_{EP}/(R_{SN})_{TH}$
^{80}Br	617.0	12200	221.3	55.13	42600	263.9	161.4	2.93
^{56}Mn	846.9	14100	199.3	70.7	26600	215.4	123.49	1.75
^{27}Mg	844.0 1014.1	-	-	-	1910	253.5	7.5	-
^{66}Cu	1040.0	3160	248.1	12.7	499	196.2	2.54	0.20
^{24}Na	1368.4	18000	220.7	81.6	18500	258.8	71.48	0.87
^{42}K	1524.7	1970	232.0	8.5	5930	229.3	25.86	3.04
^{38}Cl	1642.0	12100	113.2	106.9	14100	196.3	71.83	0.67
^{28}Al	1778.9	25700	158	162.7	7150	64.66	110.58	0.68
^{49}Ca	3083.0	-	-	-	-	-	-	-

Table 12.2

BOWEN's KALE

Isotopes	Gamma-ray Energy (KeV)	Mixed S	Mixed $\sqrt{B}$	Mixed $R_{SN}=S/\sqrt{B}$	Epithermal S	Epithermal $\sqrt{B}$	Epithermal $R_{SN}=S/\sqrt{B}$	Epithermal/Mixed $(R_{SN})_{EP}/(R_{SN})_{TH}$
^{80}Br	617.0	9760	298.3	32.72	11400	213.5	53.4	1.63
^{56}Mn	846.9	36300	333.7	108.8	13200	186.8	70.66	0.65
^{27}Mg	844.0 1014.1	2930	193.5	15.14	1390	280.2	4.96	0.33
^{66}Cu	1040.0	-	-	-	3170	242.5	13.1	-
^{24}Na	1368.4	50000	326.7	153.1	16900	216.2	78.2	0.51
^{42}K	1524.7	11300	207.1	54.56	1740	202.8	8.58	0.16
^{38}Cl	1642.0	50200	268.5	186.9	11300	170.3	66.4	0.36
^{28}Al	1778.9	2050	251.5	8.15	24700	154.4	160.0	19.63
^{49}Ca	3083.0	20500	247.1	82.96	-	-	-	-

Table 12.3

(ORCHARD LEAVES)

Isotopes	Gamma-ray energy (KeV)	Mixed S	Mixed $\sqrt{B}$	Mixed $R_{SN}=S/\sqrt{B}$	Epithermal S	Epithermal $\sqrt{B}$	Epithermal $R_{SN}=S/\sqrt{B}$	Epithermal/Mixed $(R_{SN})_{EP}/(R_{SN})_{TH}$
^{80}Br	617.0	3497	379.4	9.22	12200	295.4	41.3	4.48
^{56}Mn	846.9	214194	309.3	692.5	13900	197.1	70.5	0.10
^{27}Mg	{ 844.0 1014.1	-	-	-	7500	217.2	34.5	-
^{66}Cu	1040.0	-	-	-	9320	92.0	101.3	-
^{24}Na	1368.4	94518	337.1	280.4	1880	201.3	9.34	0.033
^{42}K	1524.7	2139	289.3	7.4	3220	210.2	15.32	2.10
^{38}Cl	1642.0	66897	281.6	237.6	2980	157.3	18.9	0.079
^{28}Al	1778.9	1964	263.5	7.45	29800	138.0	215.9	28.98
^{49}Ca	3083.0	1272	63.2	20.13	322	33.8	9.53	0.47

Materials. In the majority of the cases, higher signal-to-noise ratios are obtained in the epithermal results. The situation is not, however, simple since even in the epithermal activation, interference effects arising from the fast neutron spectrum are not reduced and may even become more pronounced in the determination of isotopes of low resonance integrals with the removal of the thermal spectrum.

A relative "gain" is defined in the table, being the enhancement ratio of signal-to-noise ratio obtained for a given activity under epithermal activation to that achieved under mixed flux conditions. Thus all radioisotopes in a given matrix, whose activities show a "gain" (i.e. with values greater than 1.0) would seem to favour epithermal activation determination rather than mixed. The values obtained from dividing the total peak area by sample mass do not reveal any easily recognizable pattern in general, although in some cases there are more counts per unit mass in the epithermal results. This is however, expected as the two samples involved in each case were not exactly identical either in mass (i.e. weight) or size, largely because the pelleting process could not be easily reproduced. This factor could influence this parameter and possibly account for the random distribution of these values as effects arising from self-shielding in the samples and to a lesser extent flux gradients in the reactor core are more likely to be amplified when viewed at the milligram level. It is, however, possible that surface contamination of the samples during preparation would have occurred and this more than the former would have serious effects on the results. Perhaps the most obvious distinction between the two methods in the results is the great improvement in the reduction of interference between ^{56}Mn and ^{27}Mg with respect to their close-lying gamma-ray energies at 846.9 KeV and 844.0 KeV respectively. The two gamma-rays (844.0 and 1014.1 KeV) of ^{27}Mg

both appeared in epithermal irradiations, whereas only the 1014.1 KeV was observed in the thermal irradiation in Bowen's Kale. And this is certainly due to the fact that there is a higher concentration of Magnesium in Bowen's Kale (1572) ppm) compared to Manganese (14.7 ppm) so that the more abundant isotope (i.e. ^{27}Mg) in the sample generated the dominant activity in the energy region of the two gamma-rays (i.e. 844.0 and 846.9 KeV). Perhaps a more serious problem posed by the total background interference is the masking of low energy peaks which lie in the neighbourhood of the Compton distribution from high energy gamma-rays. In particular, if the low energy peak is located several channels from energetic gamma-rays, then the Compton edge and/or the escape peaks from the high energy gamma-rays may completely mask the desired peak and render it undetectable. This effect is clearly demonstrated in the case of ^{66}Cu at 1040.KeV in NBS 1571 (Orchard Leaves) where serious interference from the Compton distribution of 1368.4 KeV ^{24}Na gamma-rays prevented the detection of 1040.KeV ^{66}Cu peak in mixed irradiation. This peak (i.e. 1040.KeV) was, however, identified when the sample was irradiated under Cadmium Cover. In fact, this interference effect can be estimated by merely obtaining the relative magnitude of the total background summed in the channels spanning the 1368.4 KeV ^{24}Na peak in the two irradiations. Thus, in the mixed flux, a total of 113,626 counts for the background were obtained as opposed to 40,541 counts in the epithermal spectrum. It is precisely for the same reason that Copper at 1040.KeV was not seen in Bowen's Kale in the mixed flux. In all epithermal irradiations this effect is greatly reduced, since ^{23}Na does not activate significantly in the epithermal region

The absence of ^{49}Ca at 3083.0 KeV peak or in fact at the higher energy peak of 4073 KeV in Bowen's Kale is mainly due to the low activation cross section of the isotope in the epithermal spectrum ($\sim$·32 barns) as opposed to the thermal activation cross section (1·1 barns). Clearly then, for neutron activation analysis where detection sensitivities ultimately depend on background activities generated by the matrix, the ability to suppress the total background activity and simultaneously ehancing that due to the radionuclides of interest is one of the outstanding considerations for epithermal neutron activation method.

In epithermal multielemental activation analysis, the basic quantity of interest is the "Advantage Factor" (F_a) which describes the ease with which a particular activity of interest can be determined in the presence of another interfering activity. In this work the Advantage Factors were calculated for the elements determined in the three Reference Materials and table 13 shows the results. The values were obtained by using equation 15 and 16 relative to ^{24}Na which exhibits a $^{1}/_{v}$ behaviour in the epithermal region and also being one of the most abundantly produced radionuclides present in biological materials. The table also contains calculated values of R_{Cd} (cadmium ratios) ratios for these nuclides and the $^{I'}/_{\sigma_o}$ (resonance integral to thermal cross section) ratios. From the table, it is observed that those isotopes with large $^{I'}/_{\sigma_o}$ ratios have associated with them small values of R_{Cd} ratios. The most notable in this respect are the two halides i.e. ^{38}Cl ($^{I'}/_{\sigma_o}$= 32.56, R_{Cd} = 1.64) and ^{80}Br (I'/σ_o = 18.66, R_{Cd} = 2.12). At the other extreme, ^{28}Al and ^{24}Na show exactly the opposite of the above nuclides in these properties with R_{Cd} for ^{24}Na being 39.34 and that for ^{28}Al being 27.84; whereas their $^{I'}/_{\sigma_o}$ ratios are ·543 and ·78 respectively. A plot of $^{I'}/_{\sigma_o}$ against R_{Cd} for various nuclides is shown in figure **8** . Since ENAA is used to suppress the activity of nuclides of low $^{I'}/_{\sigma_o}$ values (i.e. nuclides such as

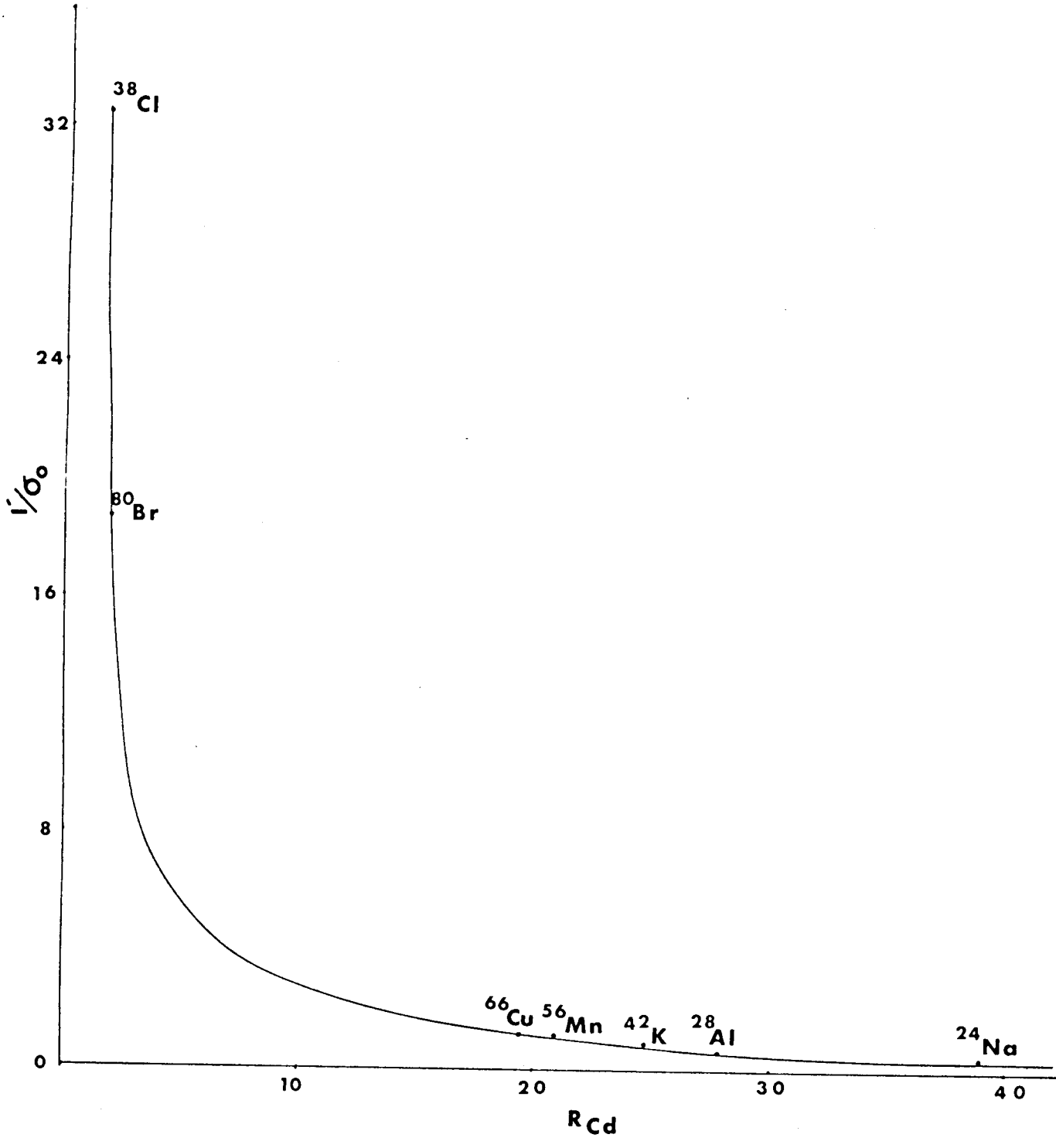

FIG 8

Na, Cu etc), in favour of nuclides of high I'/σ_o ratio, consideration of these factors in conjunction with Advantage Factors (F_a) is obviously crucial in arriving at optimal choice for ENAA work. In practice, nuclides with the F_a values greater than 1.0 favour epithermal activation. In fact, all the isotopes listed in the table (table 13) are found to have F_a values greater than 1.0 when compared to ^{24}Na, which means that epithermal activation determination of these nuclides can be performed in the presence of activities due to ^{24}Na or for that matter, any other $1/v$ nuclide with similar properties.

Sources of errors :

The accuracy and precision in epithermal activation measurements is in general influenced by a number of errors arising mainly from interfering nuclear reactions. In addition to the statistical error due to the randomness of the counting, interfering activities from threshold reactions (i.e. (n,p) and (n,α)) usually present a more serious problem in the case of epithermal neutron activation analysis than in the mixed flux, because the rate of these reactions is not lowered by the introduction of Cadmium. It has been estimated (21) that the magnitude of interference, compared to activation without Cadmium cover is higher by a factor equal to the R_{Cd} of the nuclide leading to the (n,γ) product being interfered with. The second type of error is due to interference from second order reactions of the type :

$$ {}^{A-1}_{Z-1}X(n,\gamma){}^{A}_{Z-1}X \xrightarrow{\beta^-} {}^{A}_{Z}Y(n,\gamma){}^{A+1}_{Z}Y $$

If element No. Z is being determined, the interference effect from this reaction will in general not be the same as in the case of mixed flux (Predominantly thermal) activation. The ratios of I/σ_o for the nuclides

Table 13

Radioisotope	$T_{\frac{1}{2}}$	σ_0 (barns)	$I' = I + .44\sigma_0$ * (barns)	Rcd	I'/σ_0	Fa (Relative to ^{24}Na)
^{24}Na	15.0hr	.534	.29	39.34	.543	1.0
^{27}Mg	9.5min	.030	-	-	-	-
^{38}Cl	37.2min	.43	14	1.64	32.56	23.98
^{49}Ca	8.7min	1.1	-	-	-	-
^{42}K	12.4hr	1.1	.96	24.86	.87	1.58
^{56}Mn	2.58hr	13.3	14	20.78	1.1	1.89
^{66}Cu	5.1min	2.3	2.6	19.42	1.13	2.03
^{28}Al	2.3min	.232	.18	27.84	.78	1.41
^{80}Br	17.6min	8.2	153	2.12	18.66	18.56

* $.44\sigma_0 = 1/_v$ tail

$^{A-1}_{Z-1}X$, $^{A}_{Z-1}X$ and $^{A}_{Z}Y$ usually determines the magnitude of the difference. A third possible error is the presence of many light nuclides in the sample such as ^{1}H which will moderate the neutrons within the sample giving rise to errors due to distortion of the epithermal spectrum, if the standard materials have different composition regarding light elements. The fourth type of error, and perhaps the most important in epithermal neutron activation analysis (ENAA) is that associated with self-shielding due to resonance absorption in the sample. There are two classes of this error, depending on whether or not any of the more abundant elements in the sample have resonances overlapping those of the elements to be determined in the energy region of interest. The second class includes those shielding effects dependent only on the resonances of the element being determined. In this work it was not possible to investigate the extent to which these errors influenced the overall accuracy and precision of the results obtained. It must be pointed out, however that evaluation and determination of these errors in ENAA is a sufficiently significant problem which on its own would constitute a research programme.

4.3 Analysis of biological specimens - hair samples

Analysis of biological materials for elemental content forms one of the most important practical applications of neutron activation analysis. There are many applications of elemental analysis of biological materials of which some major ones are shown in the block diagram of figure 8. In principle, any specimen from a given biological entity can be used to establish the elemental status in that species. In practice, however the use of certain specimens is limited due to a number of problems including sampling and the extent to which they reflect the total body elemental content. Hair, on the other hand is relatively easy to collect and because it is biologically inert (at least after growth) it retains a chronological

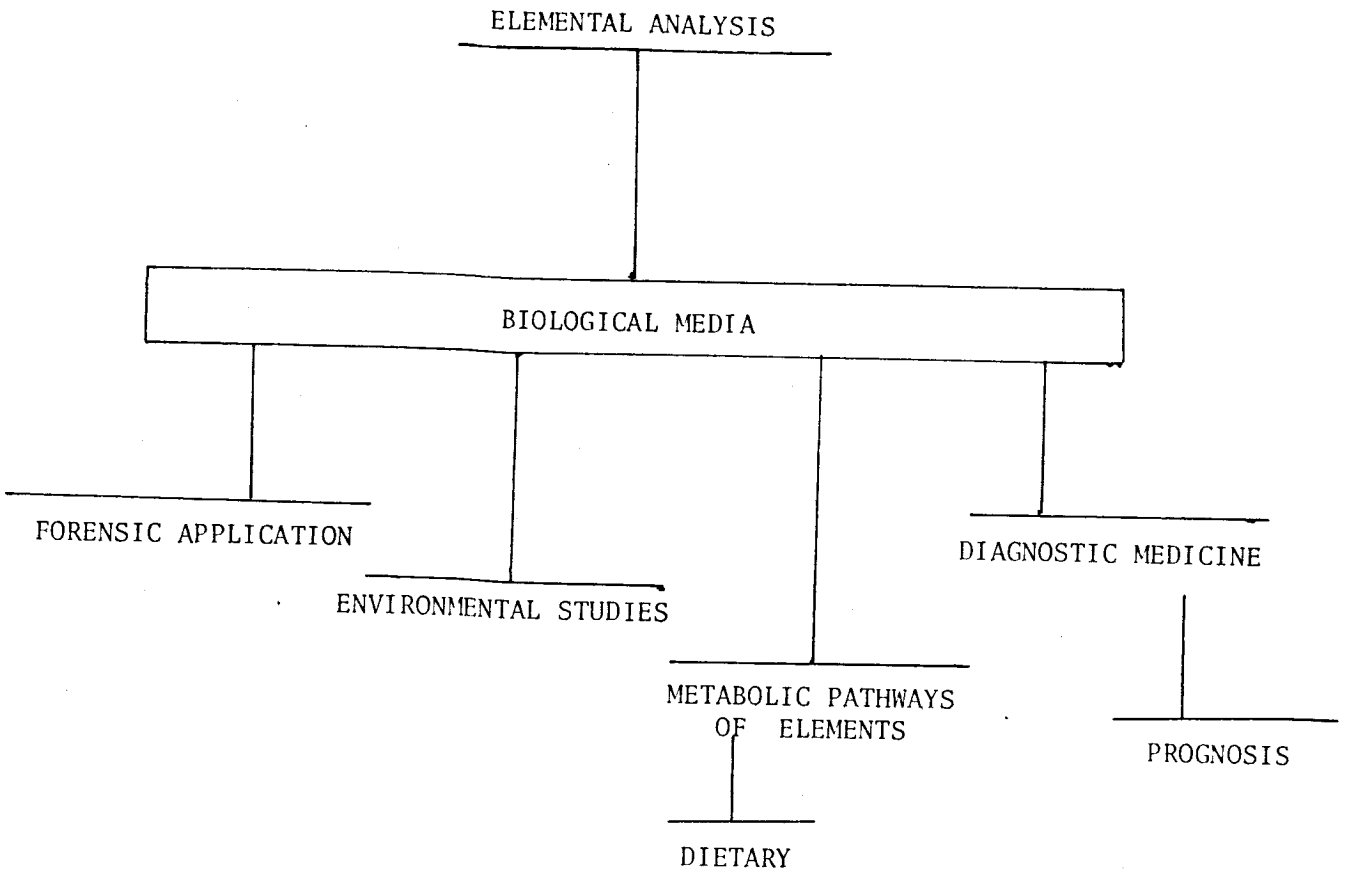

FIG.**8** APPLICATIONS OF ELEMENTAL ANALYSIS IN BIOLOGICAL MEDIA

signal of elemental intake in the species in a particular geographical region over extended periods. It is for these reasons that hair is most widely used in the determination of elemental concentrations (31).

The principle motivation for the analysis of hair samples in this work was not however, to do with any specific problem associated with any application, but rather to demonstrate the practical feasibility of Instrumental Neutron Activation Analysis technique for the assay of elemen in biological materials using short-lived activities.

4.3.1 Sample Preparation and Reactor irradiations

Hair samples belonging to children were collected from a local population in the Guildford area, Surrey (U.K.) and presented for neutron activation analysis. The preparation of hair samples involves proper cleaning of the hair so as to remove or reduce errors in the measurements arising from surface contamination. The choice of a suitable cleaning procedure usually presents a problem in that elements may be removed (30) from hair or in fact added to hair during the cleaning process. Although there are many cleaning procedures (31) most of them using different solvents for removing surface contamination, hair in this work was simply placed in an ultrasonic bath of distilled, de-ionised water and agitated for one hour, rinsed with distilled, de-ionised water and left to dry over-night in a laminar flow hood at 25°C. It was then placed in clean thin-walled low density polyethylene capsules which were in turn placed in anothe capsule and heat-sealed ready for I.C.I.S. irradiation. The cleaning metho described above was proposed and used in reference (31) where it was found to be effective in removing surface contamination from the hair with minimum loss of matrix elements.

The irradiation and counting facilities of the University of London

Reactor Centre were used in this exercise as well. Essentially, the analysis procedures were the same as those followed in the analysis of N.B.S. and other Reference Materials (see Section 4.1.1). Ten samples were irradiated for 20 minutes in the I.C.I.S. pneumatic transfer tube of the reactor at a thermal neutron flux of $1.7 \times 10^{12} n.cm^{-2}s^{-1}$. Samples were quickly transferred into clean polyethylene vials immediately after irradiation, allowing for a waiting period of 2 minutes before the start of counting. They were then counted at a constant fixed geometry of 0.5 mm above the surface of the detector (·5 mm being the thickness of the standard Whatman filter paper). The same Ge(Li) detector with the associated electronics used in the analysis of Reference Materials was also used here with the same standard settings. Samples were counted for 10 minutes and spectra collected on magnetic tapes. The tapes were later sent to the University of London Computing Centre for processing with the program "SAMPO".

4.3.2 Results and discussion

Table 14 gives a summary of the results obtained from the analysis of the spectral data using "SAMPO". The table includes the calculated gamma-ray energies corresponding to the peaks found in the spectrum for each hair sample. Also included, are the peak areas and the estimate of the uncertainty as computed by the program. The energies of the escape peaks and their areas have also been added to the table. Using the Nuclear Data Library of Subroutine "IDENT" (23), it was then possible to identify and assign the isotopes to these gamma-ray energies as illustrated in the table. From the table, at least 10 different isotopes would seem to have been successfully identified under the irradiation and counting conditions adopted. These are ^{80}Br, ^{128}I, ^{38}Cl, ^{56}Mn, ^{66}Cu, ^{24}Na, ^{28}Al, ^{49}Cu, ^{37}S and ^{76}As. The distribution of these isotopes in the samples is as follows:

Table 14

Observed E_γ (KeV)	Isotope	$T_{\frac{1}{2}}$	Hair Samples	PS1	PS2	PS3	PS4	PS5	PS6	PS7	PS8	PS9	PS10
			Mass mg	50.1	20.7	41.1	89.9	23.6	.89	.76	16.2	49	14.1
443.0	^{128}I	25.3min		-	309 (11)	445 (21)	2630 (11)	874 (14)	122 (11)	-	3830 (6)	-	-
511.0	annih.	-		14100 (.9)	2320 (1.6)	12500 (1.2)	163000 (1.23)	13700 (1.0)	260 (6.3)	302 (5)	6720 (6)	14300 (11)	9490 (1.3)
526.5	^{128}I	25.3min		-	-	-	-	-	-	-	332 (18)	-	-
554.2	^{82}Br	35.8hr		-	-	-	6850 (2.5)	-	-	-	-	-	-
559.3	^{76}As	26.4hr		-	-	-	-	-	-	74 (12)	-	-	-
617.0	^{80}Br	17.6min		5510 (4.3)	2320 (1.6)	5250 (3.8)	112000 (4.6)	13700 (4)	-	-	1970 (5.3)	6500 (3.7)	2720 (5.2)
621.0	^{38}Cl (DE)	-		1180 (16)	-	791 (18)	-	1680 (8.4)	-	-	578 (14.5)	1720 (11)	-
639.8	^{80}Br			-	-	-	3990 (42)	-	-	-	-	-	-
666.4	^{80}Br			734 (9.7)	-	698 (8.8)	19400 (12.3)	1680 (8.4)	-	-	-	1720 (11.3)	-
698.0	^{82}Br			-	-	-	2100 (5.8)	-	-	-	-	-	-
704.0	^{80}Br			-	-	-	7170 (3.9)	-	-	-	-	-	-
828.3	^{82}Br			-	-	-	1700 (10)	-	-	-	-	-	-
846.9	^{56}Mn	2.58hr		1110 (8.7)	325 (8.9)	2740 (6)	2420 (7.8)	5480 (5.3)	260 (6.3)	-	762 (8.9)	-	646 (15)

Observed E_γ (KeV)	Isotope	$T_{\frac{1}{2}}$	Hair Samples	Peak areas/(± % error)									
				PS1	PS2	PS3	PS4	PS5	PS6	PS7	PS8	PS9	PS10
			Mass mg	50.1	20.7	41.1	89.9	23.6	.89	.76	16.2	49	14.1
1040.0	^{66}Cu	5.1min		1280 (5.4)	173 (10.8)	804 (7)	18900 (3.1)	1120 (7.3)	-	-	-	659 (13)	582 (11)
1131.0	^{38}Cl (SE)			-	-	-	-	604 (9.8)	-	-	-	993 (6)	-
1145.0	^{38}Cl (DE)			6520 (1.6)	528 (5)	4300 (2.2)	5430 (2)	7500 (1.1)	-	-	2860 (2.4)	9760 (1.2)	6130 (11.2)
1255.7	^{80}Br			-	-	-	687 (8.6)	-	-	-	-	-	-
1316.6	^{82}Br			-	-	-	1000 (6.7)	-	-	-	-	-	-
1368.4	^{24}Na	15.0hr		-	854 (4.9)	4740 (2.1)	10800 (1.4)	-	-	-	2860 (2.4)	1000 (16.8)	525 (13)
1474.4	^{82}Br			-	-	-	471 (13)	-	-	-	-	-	-
1642.0	^{38}Cl	37.2min		32700 (.9)	2530 (2.7)	27200 (.9)	20500 (1.4)	37800 (.9)	361 (6.3)	464 (4.5)	361 (4.9)	14700 (1.0)	50,000 (1.1)
1655.0	^{38}Cl (SE)			1660 (6.3)	-	1590 (6.4)	869 (12)	1830 (7)	-	-	825 (6.6)	-	1490 (7)
1731.0	^{24}Na (DE)				149 (10)	1030 (5)	2250 (2.7)	-	-	-	-	-	-
1778.9	^{28}Al	2.31min		708 (10)	253 (9)	1530 (4.8)	2890 (2.4)	1260 (6)	-	-	539 (8.7)	1320 (7.1)	416 (16)
2061.7	^{49}Ca (DE)			-	229 (8)	-	1310 (4)	-	-	-	-	-	-
2080.9	^{37}S (DE)			541 (8)	-	545 (9)	664 (8)	546 (9)	-	-	332 (9.6)	-	-
2166.8	^{38}Cl	37.2min		31500 (.9)	2400 (1.9)	27000 (.9)	20700 (1.3)	36500 (.84)	376 (4)	479 (3.7)	14100 (1.2)	48600 (.92)	29300 (.9)

Observed E_γ (KeV)	Isotope	$T_{\frac{1}{2}}$	Hair Samples	Peak areas/(± % error) PS1	PS2	PS3	PS4	PS5	PS6	PS7	PS8	PS9	PS10
				50.1	20.7	41.1	89.9	23.6	.89	.76	16.2	49	14.1
2242.0	^{24}Na(SE)			-	-	-	860 (5)	-	-	-	-	-	-
2572.0	^{49}Ca(SE)			-	-	-	424 (8)	-	-	-	-	-	-
2753.6	^{24}Na	15.0hr		-	369 (5)	2010 (2.5)	4550 (.9)	-	-	-	-	459 (6)	248 (10)
3083.0	^{49}Ca	8.7min		188 (9)	270 (5)	339 (7)	1870 (3.1)	380 (6)	-	-	208 (7.3)	-	255 (8)
3102.0	^{37}S	5.1min		643 (3)	192 (7)	621 (4.4)	973 (5)	795 (4)	-	-	405 (5)	559 (6)	501 (5)

Sample 1Ps contains all isotopes but ^{128}I, ^{76}As and ^{24}Na. Samples 2Ps, 3Ps and 4Ps have all the isotopes except ^{76}As. In samples 5Ps and 9Ps all other isotopes are present minus ^{24}Na and ^{128}I respectively; whereas ^{76}As is absent in both samples. Samples 6Ps and 7Ps were unique in that very few strands of hair were irradiated, and consequently produced low intensity activities. However, ^{128}I, ^{56}Mn and ^{38}Cl were seen in sample 6Ps whereas ^{38}Cl and ^{76}As were present in sample 7Ps and the rest of the isotopes were absent. Sample 10Ps has ^{128}I and ^{76}As missing and sample 8Ps has both ^{76}As and ^{66}Cu absent.

To obtain relative concentration levels in the samples of the precursor isotopes, the areas under the peaks will have to be divided by the mass of the samples and the counts/unit mass normalized. However, the use of a comparison standard when available would enable direct conversion of the peak areas into elemental mass of the isotopes detected. In this work, NBS 1571 (Orchard Leaves) was used as the irradiation standard being one of the most representative of biological Reference Materials. Thus after correcting the peak areas for decay, dead-time and waiting period, and mass the results of elemental mass concentrations for the isotopes detected in all samples were obtained (see table 15). The success of the mass calculation of the neutron activation product isotopes depends on the presence of the activities of corresponding isotopes in the Standard Reference Material used. Thus, in this case, it was not possible to quantify Iodine, Sulphur and Arsenic due to the absence of the corresponding activities of these isotopes in the Standard.

The results presented in table 15 are from a Preliminary survey of Neutron Activation Analysis of hair samples using short-lived activities in a single experimental run. Thus, in order to be able to confirm the accuracy and precision in the results obtained, it would require a series

Table 15

Element	Isotope	$T_{\frac{1}{2}}$	γ-ray used (KeV)	sample No.	1PS	2PS	3PS	4PS	5PS	6PS	7PS	8PS	9PS	10PS
				mass	50.1mg	20.7mg	41.1mg	89.9mg	23.6mg	.899mg	.766mg	25mg	49.0mg	50.0mg
Bromine	^{80}Br	17.6min	617.0	ppm	15.0 (1.03)	1.92 (.14)	14.3 (.93)	3989 (307)	14.3 (.10)	-	-	5.8 (.5)	24.5 (1.8)	8.8 (0.7)
Manganese	^{56}Mn	2.58hr	846.9	ppm	.41 (.06)	.10 (.01)	.99 (.1)	1.1 (.1)	2.4 (.2)	0.03 (.001)	-	.25 (.03)	-	.23 (.03)
Copper	^{66}Cu	5.1min	1040.0	ppm	901.4 (21)	102.5 (14)	557.8 (61)	15663 (1505)	837 (98)	-	-	333.8 (42)	531.8 (85)	403.7 (58)
Sodium	^{24}Na	15.0hr	1368.4	ppm	-	.72 (.1)	4.6 (.2)	12.6 (.4)	-	-	-	.33 (.03)	1.14 (.2)	.52 (.1)
Chlorine	^{38}Cl	37.2min	1642.0	ppm	398.5 (13)	25.3 (.7)	317.9 (4)	286 (5)	476 (7)	3.55 (.2)	4.6 (.2)	157.2 (2.0)	680 (75)	352.9 (5)
Aluminium	^{28}Al	2.31min	1778.9	ppm	8.4 (.9)	2.5 (.3)	17.9 (1.6)	40 (3)	17.6 (2.0)	-	-	5.8 (.6)	18.0 (.18)	4.9 (.9)
Calcium	^{49}Ca	8.7min	3083.0	ppm	430 (43)	4300 (210)	6300 (340)	41600 (3000)	8500 (800)	-	-	6500 (580)	-	4700 (488)

of measurements made on the same samples under reproducible irradiation and counting conditions. It is mainly for this reason that the results in table 15 can only be used as indicators for the presence of these isotopes in the samples analyzed. Further analyses would help to confirm the presence and facilitate accurate quantification of the isotopes. The exercise has, however, demonstrated the practicality of determining element in biological materials using short-lived instrumental neutron activation analysis. The results obtained are compared with some average (mean) values from other studies in a variety of populations (31, 37, 38).

4.4 Prompt gamma-ray spectrometry using Am/Be - neutron source

The analytical sensitivity of the prompt gamma-ray technique depends on the neutron absorption cross section (σ barns), and on the capture gamma-ray yield Y(which can be defined as gamma-rays emitted per 100 neutrons absorbed). Some elements such as Boron and Cadmium have very large thermal neutron capture cross sections; thus, it is feasible to measure micrograme quantities of these elements using this method. However, most elements do not possess large cross sections, so that milligram quantities are usually required to produce detectable lines in the prompt gamma-spectrum. For any element, the product $Y\sigma/A$, where A is the mass number defines an index of sensitivity.

4.4.1 Large body experiments

On the basis of sensitivities available in reference 32, it was decided to analyse some elements in various chemical compounds (mainly Analytical Reagents) with the Am/Be as the neutron source. Thus, it was hoped to characterize those chemical compounds by establishing significant spectral lines and their relative response and consequently calibrate the experimental assembly.

(i) Irradiations and counting

Samples of powdered Sulphur (S), Copper Sulphate ($Cu\ So_4$), Ferric Oxide (Fe_2O_3), Magnesium Oxide (MgO), Manganese dioxide (MnO_2) and Sodium Carbonate (Na_2CO_3) were placed in clean polyethylene vials and weighted ready for beam irradiation. The irradiations were carried out in the Departments' 5Ci (University of Surrey Physics Department) Am/Be - neutron source. The source is housed in a double-walled perspex cylindrical capsule of approximately 5 cm diameter and 10 cm long. The source capsule is placed inside a long cylindrical tube made of perspex which forms the beam collimation tube. The source is moved from the rest position to the irradiation position and vice versa by means of a pneumatic transfer system which allows for both single and cyclic irradiations to be carried out. The entire assembly is placed in a storage tank filled with water which also acts as the reflector and biological shield (see diagram 2). The source has a thermal flux of $5 \times 10^4 n\ cm^{-2} s^{-1}$. Gamma-ray spectra were collected with an ORTEC 100 cm^3 Coaxial Ge(Li) detector coupled to a Spectroscopy Canberra Amplifier Model 1413, Northern Ns-623-8192 ADC 1000 channels MCA. Spectra were analysed and output through an on-line Computer-based system (LINK SYSTEM 290) which has facilities for automatic linear background subtraction, visual-display (VDU) and floppy disk (diskette) storage of spectra. The system resolution is 1.95 KeV (FWHM), a peak to Compton ratio of 36:1 and a counting efficiency of 10% all compared at 1332 KeV photopeak of ^{60}Co. The system was calibrated at 1.99 KeV / channel using 1332 and 1173 KeV gamma-rays of ^{60}Co standard source (see figure 9 for Calibration Spectrum). For irradiation, samples were placed in a water "phantom" (to provide moderation) at a fixed geometry in the irradiation area and the source moved to the front and left there for 30 minutes. Simultaneously, the Ge(Li) detector, located at the side, shielded with lead bricks to reduce the gamma-ray

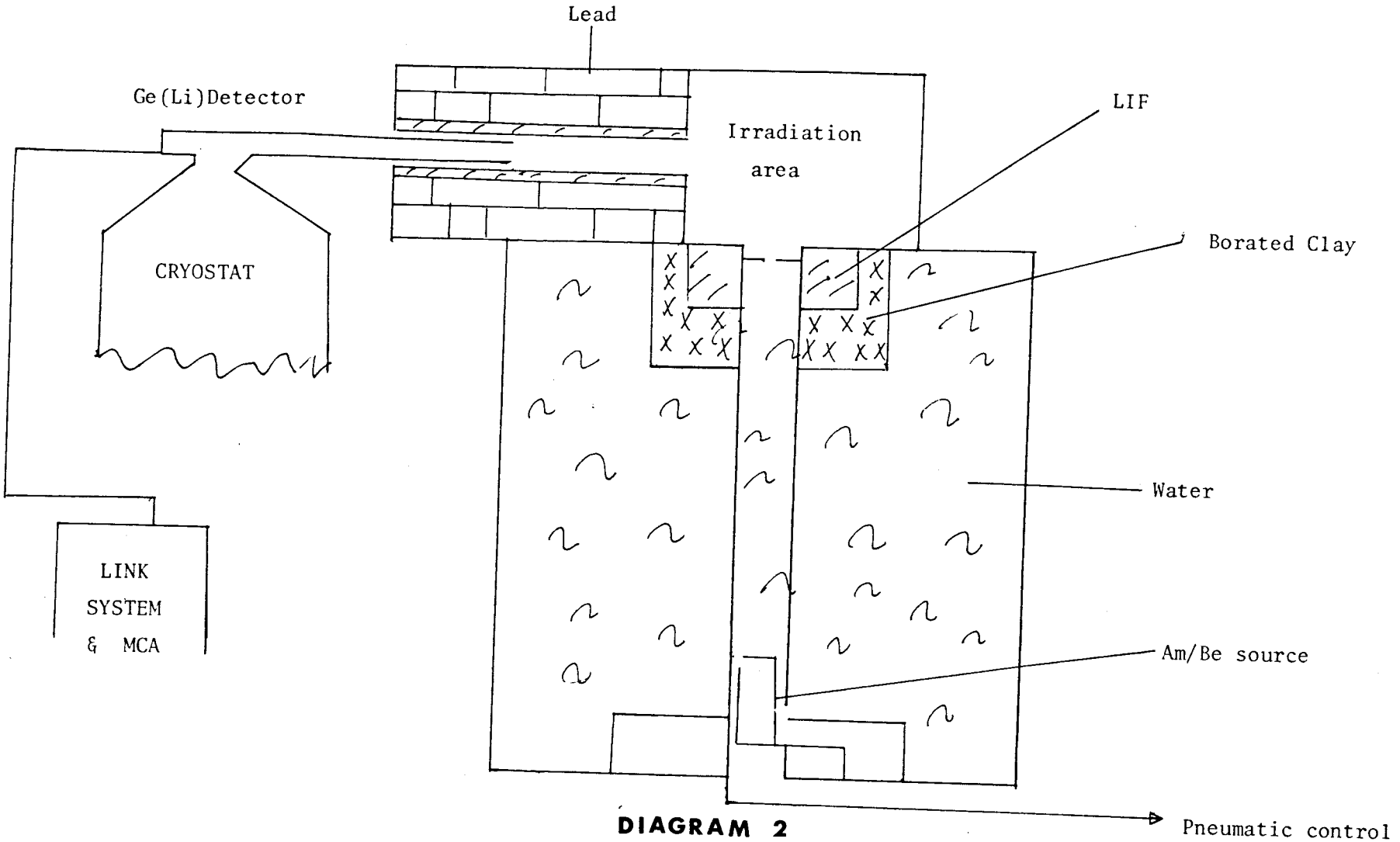

DIAGRAM 2

Experimental Assembly of Am/Be Neutron tank

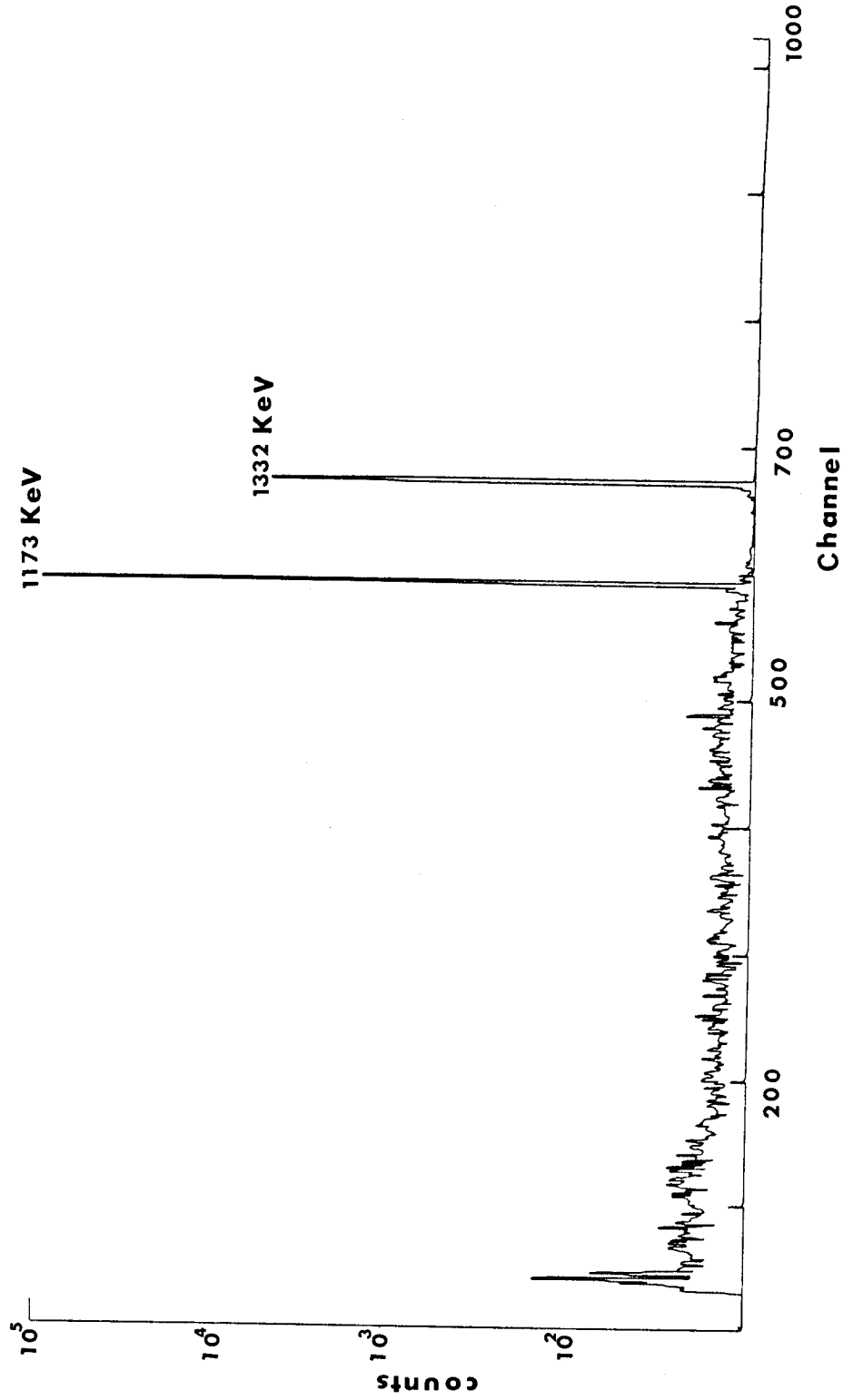

FIG 9

^{60}Co calibration spectrum

background and with Lithium Fluoride (LiF) plus Boral to reduce scattered and stray neutrons measured the gamma-rays from the sample.

4.4.2 Results and discussion

In all irradiations gamma-rays in the 0-2200 KeV energy range were measured. In principle this energy region has an advantage when compared with a higher energy range for the simple reason that sensitivities are generally high for many elements. This is true because the low-lying energy levels in excited compound nuclei produced in capture reactions are normally populated by high energy levels. However, signal-to-noise ratios in this region are usually low due to the increased contribution of scattered gamma-rays.

The spectra collected in these experiments showed serious interference from "background" gamma-rays mainly from the activation of Ge in the detector and the material around the irradiation area. Table 16 is the "background" spectrum showing detector response for the source at the irradiation position. The table also identifies the source of the various gamma-rays using the data reported in reference 33. Figure 10 shows the measured spectrum of Fe. The major peaks are the 2200 KeV Hydrogen capture line and the two escape peaks at 1709 KeV and 1199 KeV and 478 KeV Doppler broadened peak of Boron. The rest of the peaks are either due to thermal neutron capture or inelastic scattering in the detector, the lead shielding and the building material. These gamma-rays dominated the spectrum in all measurements and prevented to a large extent, detection of any gamma-rays of interest. However, in order to make an estimate of the capability of the system, the detection limits were calculated for a number of elements of interest for an irradiation time of 900 s, based on the matrix counts produced by the source.

Table 16. Background spectrum taken with source in irradiation position t_c = 900sec

Channel No.	Gamma-ray energy (KeV)	Gamma-ray source
240	478	B(n,γ)
248	494	Ge(n,γ)
251	500	Ge(n,γ)
257	511	annihilation
286	570	^{207m}Pb(0.7s)
294	585	Ge(n,γ)s.e.
301	598	Ge(n,γ)
348	693	Ge(n,n´γ)
356	708	Li(n,γ)
432	860	Pb(n,γ)
436	867	Ge(n,γ)
451	897	Pb(n,n´)
482	960	Ge(n,γ)
509	1012	Aℓ(n,n´γ)
550	1095	Ge(n,γ)
603	1199	H(n,γ)d.e.
652	1297	Fe(n,γ)
799	1590	Pb(n,n´γ)d.e.
858	1709	H(n,γ)s.e.

s.e. - single escape peak

d.e. - double escape peak

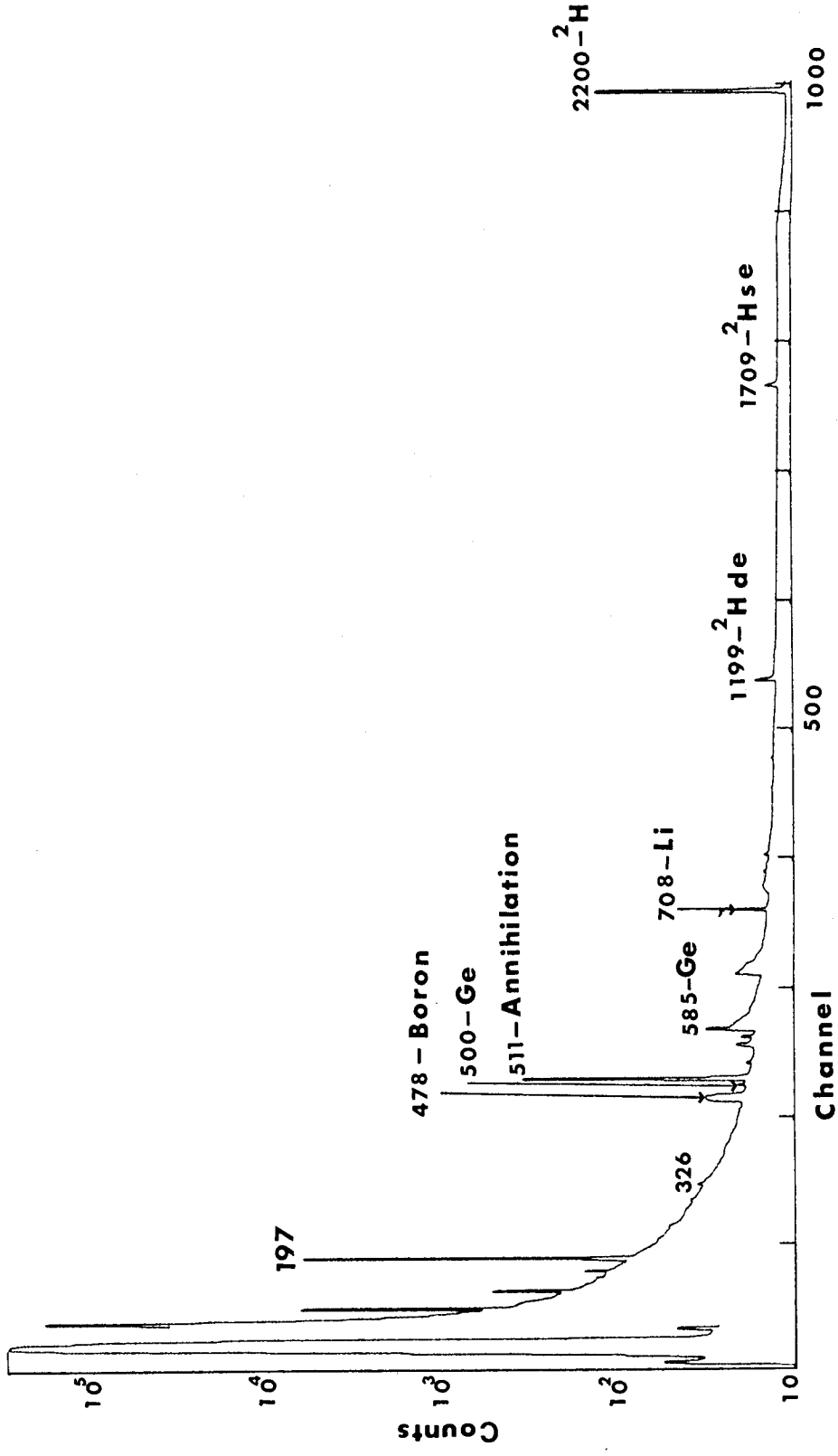

FIG 10

Capture gamma-ray spectrum of Fe

Estimation of the detection limit was based on gamma-rays with the highest index of sensitivity ($S = Y\sigma/A$) in the energy region 0 - 2200 KeV and best detection limits were determined for all cases and shown in table 17. The definition of detection limit has been assumed as the mass of the element in question which corresponds to a count of $2\sqrt{B}$ (twice the statistical deviation of the background). Thus, for any gamma-ray energy E, the background was calculated from the following equation :

$$B = \frac{1}{2}\left(\sum_{i=N-2j}^{N} n_i + \sum_{i=N}^{N+2j} n_i - n_N \right) \qquad (26)$$

where, n_i - count of the i-th channel

N - channel number corresponding to E

j - number of channels with $2\Delta E$, ΔE being the resolution of the detector (FWHM).

The values given in the table were calculated from the semi-absolute equation 9 given in section 1.3.1 and the efficiency data were obtained from reference 34. The detector efficiency curve is shown in figure 11.

The detection limit values obtained for Fe, Mg, Cu, S, Na, Ca, and Mn and indicate the feasibility of using the capture gamma-ray technique on the Am/Be source for large body measurements. As can be seen from the table Ca shows a very high value, implying a very low sensitivity. The estimate of errors enclosed in brackets was determined absolutely through the uncertainties associated with the parameters in the activation equation. The errors are found to give an accuracy of between 10-15% in the estimated values.

The use of prompt gamma-ray determination of large bodies is definitely feasible using the 5Ci Am/Be neutron source. For improved results, the total background interference must be greatly reduced.

Table 17 $t_i = t_c = 900s$

"Prompt" Activation Detection Limits determined on the Am/Be-source

Element	Matrix material	Gamma-ray energy(KeV)	Sensitivity $S = Y\sigma/A_W$	B	$2\sqrt{B}$	Detector Efficiency (E)	ppm	Sample Mass
Cu	$CuSO_4$	609.0	0.481	4608	135.8	2.96×10^{-2}	1683 (168)	20.8gm
Mg	MgO	1809.0	0.652	2112	92.0	4.73×10^{-3}	1833 (183)	6gm
Fe	Fe_2O_3	353.0	0.509	5987	154.8	4.86×10^{-2}	2300 (230)	10gm
Na	Na_2CO_3	870.0	0.590	2111.5	91.9	1.97×10^{-2}	3452 (518)	8.4gm
S	Powder	841.0	0.867	4247.5	130.4	2.1×10^{-2}	4369 (612)	5.95gm
Mn	MnO_2	314.0	0.859	6852	165.6	2.45×10^{-2}	9660 (1352)	3gm
Ca	$CaCO_3$	1943	0.563	982	62.7	3.86×10^{-3}	29258 (3803)	3.64gm

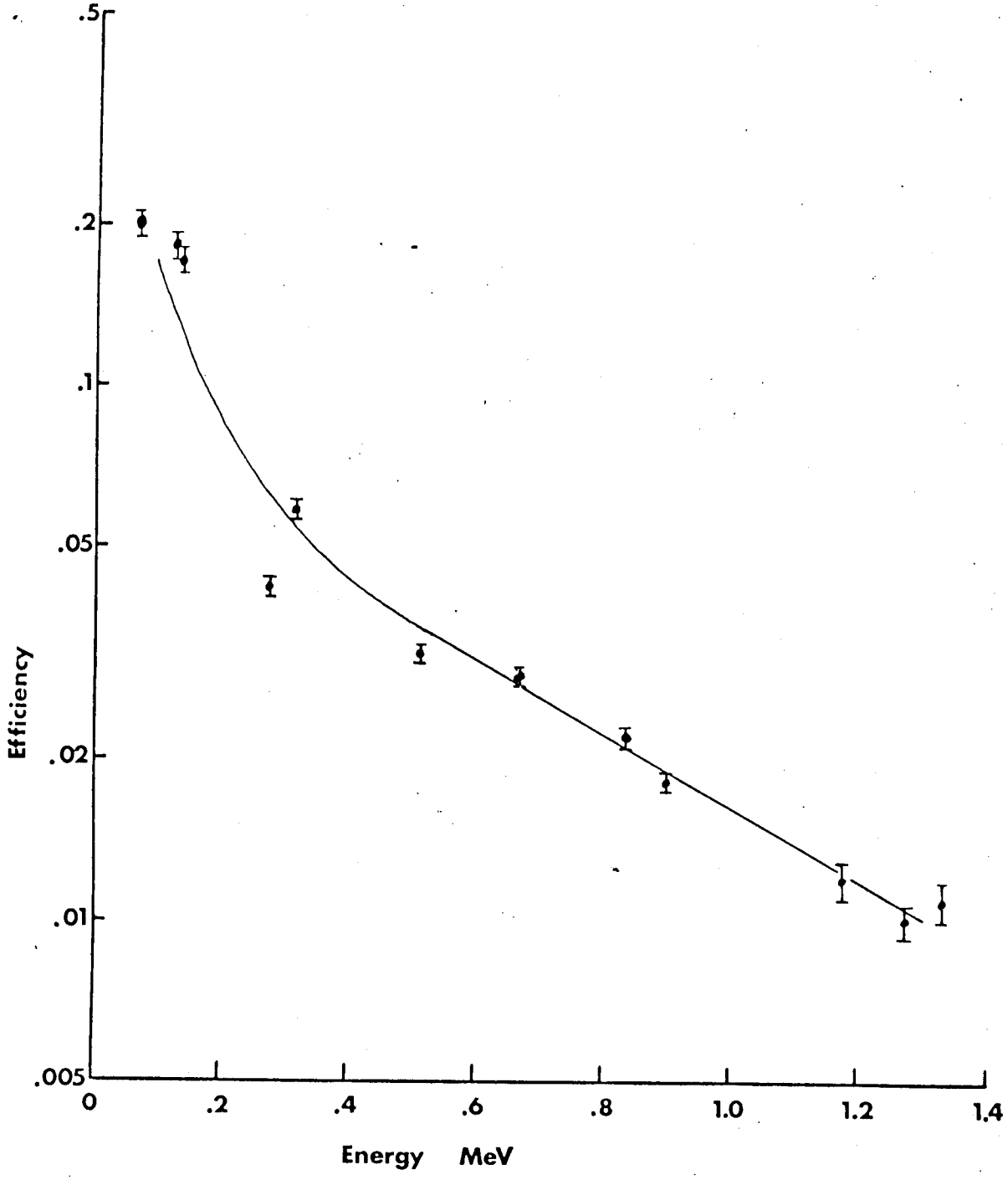

FIG 11

Ge(Li) detector efficiency as a function of gamma-ray energy

The method is economical in time, since measurements are made during irradiation and it is possible to measure many elements when they are present as major or minor constituents in a variety of matrices. The technique is non-destructive and cost effective if the required facility is available. Possible areas of application include process control in industries, medical applications based on invivo measurements of minor or major elements.

CHAPTER 5

5. CONCLUSIONS

The performance of any analytical technique used for elemental determination is evaluated in terms of three basic factors. These are (1) Selectivity (2) Sensitivity and (3) Speed. Selectivity is the ability to detect and determine one element in the presence of other elements with special reference to those other elements which are commonly associated with the desired constituent and which might be expected to interfere with its identification and determination. Sensitivity on the other hand, means the smallest amount of the desired element which will give a satisfactory signal with the particular technique being used. And Speed is how soon are the analytical results available. Instrumental Neutron Activation Analysis (INAA) is gaining increased popularity in elemental determination because of its significant contribution to these three factors. The method is selective in that the process of activation involves only the nucleus and thus independent of the chemical state of the element in question. The nuclear reaction is simple which means that nuclear properties of the isotopes (e.g. half-life, type of disintegration etc) can be well characterized giving rise to positive identification of the precursor isotopes. With the use of Ge(Li) detectors, the method allows simultaneous analysis of a number of elements non-destructively. INAA has probably the highest sensitivity as an analytical technique. Many elements can be determined in the part per million (ppm) or even part per billion (ppb) by activation with high flux reactor neutrons ($\sim 10^{12} ncm^{-2} s^{-1}$). The sensitivity can be further enhanced by the use of specialized techniques such as cyclic activation analysis. The technique offers the greatest gain in time and analytical results can be obtained almost instantaneously in the case of "prompt" activation analysis.

If the delay mode is used, the determination of elements usually involves the time allowable between removal from the activating reactor and the counting of the induced activity. In the radioactivation mode, INAA is limited to those types of samples wherein the matrix does not excessively become radioactive, forms radioisotopes of very weak activity and produces short-lived radioisotopes. In general, the high cost of irradiation facilities and measuring equipment means that only relatively large specialized institutes (e.g. Universities) or industries can use the technique on a routine basis.

INAA, because of its high sensitivity is ideally suited for use in trace determinations (usually ppm). In general however, the method can be used to determine elements present in samples at any level including major and minor constituents. In fact, the determination of the latter is likely to lead to a more widespread use of INAA, with the development of smaller, cheaper and easily operated low flux neutron sources (i.e. isotopic and neutron generators).

In principle, it would be advantageous to analyse large samples (typically gm - kilogram range) for the purpose of homogeneity and representativeness. However, large samples cannot usually be analysed through the radioactivation form of INAA, owing to a number of practical problems including sample self-shielding, reactor operation and in some cases health hazards arising from induced activities and disposal of irradiated materials. To minimize these problems, it means very small samples must be used ($\sim$1 mg - 1gm) in the radioactivation mode. With the development of high resolution Ge(Li) detectors, prompt gamma-ray measurements can now be carried out in many analyses eliminating the practical limitations imposed by sample size. Additionally, the ability to measure practically all elements including those not suitable for radioactivation in particular light elements (i.e. H,C,N,B etc) is perhaps the most outstanding consideration for prompt gamma-ray spectrometry.

INAA is now an established analytical technique applied to many micro and macro element determinations in various fields. For trace element applications, the method is an invaluable tool in the fabrication of high purity materials used in semiconductors and nuclear reactor engineering where extremely minute quantities of impurity elements have to be determined. The need to determine trace constituents in biological materials so as to study their effects on the physiological process of living systems is of an extreme importance. In order to obtain information of biological interest concerning the spread and concentrations of trace elements in biological tissues large numbers of analyses have to be done both invivo and invitro. Recently some unique features of INAA have been utilized to meet specialized needs in forensic investigations. Because of the high sensitivity for many elements, it is possible to analyse minute samples (e.g. blood, nails, hair, paints, etc.) found at the site of a crime. On the other hand, macro determinations have, mainly been used in conjunction with geochemical and geological applications, in the study of elemental distributions in meteorites and lunar materials and mineral explorations respectively.

The experiments carried out in this work were an attempt to demonstrate the efficacy of using Instrumental Neutron Activation Analysis (INAA) techniques for elemental determination in a number of selected materials and I feel that this has been successfully achieved.

The results obtained in the Analysis of NBS and other Reference Materials agree favourably well with literature data, confirming the present state of knowledge in this field. The analysis of hair samples indicated the feasibility of activation based on short-lived isotopes in biological materials. In "prompt" activation, a case was established in favour of large body measurements of major and minor constituents

using a 5Ci Am/Be Isotopic Neutron Source. The results and experience gained from this work strongly suggest that the availability of well characterized materials as irradiation standards is the most feasible approach for accurate and reliable determinations using the comparator method.

In conclusion, I feel that techniques in Instrumental Neutron Activation Analysis (INAA) could be profitably used in solving a number of important problems in many fields in developing countries. In particular, "Prompt" activation determination using small, cheap and easily operated neutron sources could be efficiently used for In-Situ measurements in mineral exporation in an environment such as that of Zambia.

BIBLIOGRAPHY

1. Egan A., Spyrou N.M., J. Radioanal. Chem., 37, (1977), 775

2. SAMPO-ULCC Version, Users Manual, University of London Reactor Centre, Silwood Park.

3. Routti J.T., Prussin S.G., Nucl. Instr. and Methods, 72, (1969), 125.

4. Baedecker P.A., Anal. Chem., 43, (1971), 405.

5. Quittner P., Nucl. Instr. and Methods, 76, (1969), 115.

6. Kokta L., Nucl. Instr. and Methods, 112, (1973), 245.

7. Waibel E., Grosswendt B., Nucl. Instr. and Methods, 131, (1975), 133.

8. Pillay K.K., Miller W.W., J. Radioanal. Chem., 2, (1969), 97.

9. Robertson R., Spyrou N.M., Anal. Chem. 47, 1, (1975), 65.

10. De Soete D., Gijbels R., Hoste J., "Neutron Activation Analysis" Chapter 7.0, Wiley-Interscience 1972.

11. Givens W.W., Mills W.R., Caldwell R.L., Nucl. Instr. and Methods, 80, (1970), 95.

12. Spyrou N.M., Kerr S.A., Radioanal. Chem., 48, (1979), 169.

13. *Gladney E.S. et al, Anal. Chem. 48, 14 (1976), 2139.*

14. Dabek J.T. et al, Proc. Int. Conf. on Modern Trends in Activation Analysis, 1, (1976), 204.

15. Covell D.F., Anal. Chem., 31, 90, (1959), 1785.

16. Sterlinski A., Anal. Chem., 40, 8, (1968), 1995.

17. Curtis L.F., "Introduction to Neutron Physics", Chapter 3, Van Nostrand, 1958.

18: Anon, Nucleonics, 14, (1956), 105.

19. Spyrou et al, Proc. Second Int. Conf. on Nuclear Methods in Environmental Research, University of Missouri, (1974), 106.

20. Evans R., "Atomic Nucleus", McGraw-Hill, (1955).

21. Steins E., Talanta, 16, (1969), 1326.

22. Standard Reference Materials Catalog, NBS Special Publication 260, 1979-80 edition.

23. Carder W., Macmahon, Egan, Talanta 25, (1978), 21.

24. Lerder C.M., Hollander J.M., Perlman I., Table of Isotopes, VI Edition.

25. Nuclear Data Group, ORNL (Editors), Nuclear Data Tables.

26. Glower D., "Experimental Reactor Analysis and Radiation Measurements", McGraw-Hill, (1965).

27. Bowen H.J.M., J. Radioanal. Chem., 19, (1974), 215.

28. Nadkarni R.A. et al, J. Radioanal. Chem., 43, (1968).

29. Spyrou N.M. et al, IAEA-SM-175/20.

30. Bate L.C. et al, Nucleonics, 10, (1965), 74.

31. Othman I., Spyrou N.M., IAEA-SM-227/33.

32. Senftle F.E. et al, Nucl. Instr. and Mehtods, 104, (1972), 485.

33. Shani G., Int. J. Appl. Radiation and Isotopes, 24, (1973),519-524.

34. Matthews I., Pearson D., Private communication.

35. Glastone S., Sensoske A., "Nuclear Reactor Engineering", Van Nostrand (1967).

36. Knol G., "Radiation Detection and Measurements", John Wiley and Sons (1979).

37. Clemente G.F. et al, IAEA-SM-227/13.

38. Sakurai S. et al, IAEA-SM-227/16.

Corrigenda

Page No.

5.0 the line σ- cross section for the reaction to take place (barn) should read, σ- cross section for the reaction to take place (cm^2)

6.0 in equation 4, the symbol A, denoting the atomic weight of the element should be A_w

8.0 in the last sentence but one at the bottom of the page, the condition for T (i.e the cycle period) should read $T \geq t_i + t_w + t_c + t_{w'}$, where $t_{w'}$ is the time between end of counting and start of another irradiation run.

14.0 in equation 10, n(E) should read, the number of neutrons with energy E per unit energy interval, for each neutron emitted

15.0 the left side of equation 11 should read $\frac{dn(E)}{n}$, where dn(E) is the number of neutrons with energies in the range from E to E + dE and n is the total number of neutrons in the system.

16.0 the line σ_o- 2200 ms^{-1} neutron cross section should read, σ_o- cross section for a neutron having velocity 2200 ms^{-1}

20.0 under section (a), the sentence beginning Typical reactions include: the last reaction should be $^3H(p,n)^3He$

35.0 equation 22 should read,

$$A = na_o + \sum_{j=1}^{n} (n-j+1) - (a_{-j} + a_j) - \sum_{j=1}^{n} (j+\tfrac{1}{2}) - (b_{-j} + b_j)$$

36.0 in equation 24, the expression $F_i(p_j)$ should read $F_j(X_i)$